UC San Diego
UC San Diego Electronic Theses and Dissertations

Title

The Role of PP2Cs and PYR/PYL ABA Receptors in Calcium- Dependent Abscisic Acid Signaling

Permalink

https://escholarship.org/uc/item/4vg0j9xj

Author

Yang, Paul Geejun

Publication Date

2013

Peer reviewed|Thesis/dissertation

UNIVERSITY OF CALIFORNIA, SAN DIEGO

The Role of PP2Cs and PYR/PYL ABA Receptors in Calcium-Dependent Abscisic Acid
Signaling

and

The Development and Characterization of a FRET-based Malate Biosensor

A Thesis submitted in partial satisfaction of the requirements
for the degree Master of Science

in

Biology

by

Paul Geejun Yang

Committee in charge:

> Professor Julian Schroeder, Chair
> Professor Nigel Crawford
> Professor Yunde Zhao

2013

The Thesis of Paul Geejun Yang is approved and it is acceptable in quality and form for

publication on microfilm and electronically:

_____

_____

_____

<div align="right">Chair</div>

University of California, San Diego

2013

TABLE OF CONTENTS

LIST OF FIGURES

LIST OF TABLES

ACKNOWLEDGEMENTS

ABSTRACT OF THE THESIS

The Role of PP2Cs of PYR/PYL ABA Receptors in Calcium-Dependent Abscisic Acid

Signaling Pathway and the Development and Characterization of a FRET-based Malate

Biosensor

by

Paul Geejun Yang

Master of Science in Biology

University of California, San Diego, 2013

Professor Julian Schroeder, Chair

ABA is a phytohormone that plays a major role in plant processes and

homeostasis. ABA is a drought-induced phytohormone that regulates stomata. Stomata

are pores in the aerial epidermal tissue of plants that are responsible for the exchange of

gases, nutrient transport, and leaf cooling. In the ABA signaling pathway, PYR/PYL

ABA receptor proteins and PP2Cs regulate the downstream response of stomatal closure

in Ca^{2+}-independent and Ca^{2+}-dependent pathway. Evidence shows that ABA elicits a

downstream increase in $[Ca^{2+}]_{cyt}$ and that $[Ca^{2+}]_{cyt}$ is required for ~70% of the response. To

study the potential relationship of PYR/PYL ABA receptor proteins and PP2Cs in

calcium-dependent ABA signaling pathway, stomata were monitored after exposure to

ABA and elevated Ca^{2+} in *Arabidopsis thaliana*. PP2C mutant leaves showed

hypersensitivity to ABA and Ca^{2+}. PYR/PYL ABA receptor mutant showed no

difference, in comparison to wildtype, when exposed to high Ca^{2+}; however there was a

noticeable difference in $[Ca^{2+}]_{cyt}$ elevations when leaf epidermis were exposed to ABA.

Malate is involved in stomatal regulation by changing $[malate]_{cyt}$ in guard cells in

the presence of ABA. Building a FRET-based malate sensor would allow real-time

monitoring of malate, *in vivo*. Malate sensor was designed by isolating the malate-

binding domain of the YufLM two-component system from *Bacillus subtillis*. The sensor

protein was purified and characterized based on the emission spectra, the binding affinity

of the sensor to malate, and unspecific binding of other structurally similar substrates.

Evidence shows that this malate sensor could potentially be used, in vivo, for future

experiments.

I.

The Role of PP2Cs and PYR/PYL ABA Receptors in Calcium-Dependent Abscisic Acid Signaling Pathway

1.1. Abstract

Abscisic acid (ABA) is a phytohormone that allows plants to respond to abiotic stresses such as drought, heat, humidity, ozone, and cold. Over the past three decades, the ABA signaling pathway was investigated; however many of the key regulatory components are still unclear. In the core ABA signaling pathway, both a calcium-dependent and –independent pathway converge to elicit downstream events including stomatal closure. It has been shown that Ca^{2+} acts as a major part of the overall ABA-induced stomatal closure pathway, proving the importance of understanding calcium dynamics in guard cells. Understanding the role of proteins involved in ABA signaling in the presence of ABA and Ca^{2+} could be helpful in elucidating the regulatory mechanisms of $[Ca^{2+}]_{cyt}$ and the plasma membrane Ca^{2+} permeable channel, I_{Ca}. A family of START-domain proteins, PYR/PYL/RCAR, and PP2C, protein phosphatases, are key components of the ABA signaling pathway. Calcium transients and stomatal closing indicate that these two components of the ABA signaling pathway could be crucial to the regulation of the I_{Ca} and $[Ca^{2+}]_{cyt}$.

1.2. Introduction

Stomata are adjustable openings in the epidermis of leaves that allow the exchange of gases such as O_2 and CO_2. Stomata offer the plant protection from water loss due to evaporation. The opening and closing of stomata is influenced by a variety of environmental factors, including, but not limited to: humidity, light, temperature, ozone, and phytohormones (Schroeder et al., 2001; Raschke et al., 1988). The stomate is composed of two specialized guard cells that close and open stomatal pores by regulating turgor pressure (Schroeder et al., 2001). Although plants have adapted to overcome environmental stress, abiotic stresses have significantly affected crop yield (Morgan, 1984; Epstein et al., 1980; Ingram and Bartels, 1996).

Abscisic acid, ABA, is a drought-induced phytohormone that is crucial for many plant functions including seed germination, root development, flowering, seed maturation, drought resistance, seed dormancy, and root growth inhibition (Acharya et al, 2009; Himmelbach et al., 1998; Kim et al., 2010; Santner et al., 2009; Schroeder et al., 2001; Deak and Malamy, 2005; Rodriguez et al., 2009). Over the past three decades, the role of ABA in stomatal regulation has been studied, and major components of the calcium-independent ABA signaling pathway have been identified. Families of proteins involved in the calcium-independent ABA signaling pathway include: ABA receptor proteins named PYR (pyrabactin resistance), PYL (pyrabactin like), RCAR (regulatory component of ABA receptor), PP2Cs (2C type Protein Phosphatases) including ABI1 (ABA insensitive), ABI2, PP2Ca, and HAB1 (Homolog to ABI1), a family of Serine/Threonine kinases (SnRK2s) including OST1 (open stomata 1), and, finally, downstream targets including the anion channel SLAC1 (reviewed in Kim et al., 2010).

The proposed model suggests that ABA binds to the family of ABA receptor proteins (PYR/PYL), which forms a complex (Park et al., 2009; Nishimura et al., 2009; Nishimura et al., 2010). The ABA receptor complex binds and inhibits the family of PP2Cs (Park et al. 2009; Nishimura et al. 2009; Nishimura et al. 2010), which dephosphorylates and inhibits the activity of SnRK2s (Umezawa et al. 2009; Vlad et al. 2009). The phosphorylated SnRK2 protein kinases induce downstream effects of ABA including phosphorylation of SLAC1, the major anion channel in guard cells (Negi et al., 2008; Vahisalu et al., 2008; Geiger et al. 2009; Geiger et al. 2010; Vahisalu et al. 2010, Brandt et al., 2012). In summary, ABA closes stomatal pores by downstream events - the efflux of ions and also by gluconeogenic conversion of malate into starch, which leads to a decrease in turgor pressure (MacRobbie 1998; Schroeder et al., 1987; Schroeder and Hagiwara 1989; Vahisalu et al., 2008).

The PYR/PYL/RCAR family encodes START-domain proteins in the ABA signaling pathway and shares a hydrophobic ligand-binding domain with a barrel and lid structure for the binding of ABA (Nishimura et al., 2009; Santiago et al., 2009). Upon binding of ABA, conformational changes allow the exposure of a hydrophobic domain, which binds to the active site of PP2Cs (Melcher et al., 2009; Miyazono et al., 2009; Yin et al., 2009). A large family of START proteins in the ABA signaling pathway have been identified. A 14 gene family PYL1-PYL14 and an identical RCAR1-RCAR14 family have been identified. It is known that the function of the START proteins in the ABA signaling pathway are important for inhibition of PP2Cs (Rubio et al., 2009). However, other functions of the START proteins are not known.

In the core ABA signaling pathway, PP2Cs function as negative regulators by inhibiting the activity of SnRK2s (Umezawa et al., 2009; Vlad et al., 2009). Although it has been shown that PP2Cs are able to regulate SnRK2s and SLAC1 activity (Brandt et al., 2012), the interactions and regulation of another family of calcium dependent protein kinases (CPKs) is less well understood. CPKs are protein kinases that are active in the calcium-dependent ABA signaling pathway due to their ability to phosphorylate downstream targets and detect calcium. They function by directly phosphorylating and activating the SLAC1 channel (Mori et al., 2006; Geiger et al., 2010; Brandt et al., 2012). CPK mutants exhibit ABA and calcium insensitivity showing that CPK mutants are downstream of or at the level of calcium sensing (Mori et al., 2006).

Intracellular $[Ca^{2+}]$, a secondary messenger, is an important signaling component that induces stomatal closure (Schroeder and Hagiwara, 1989; Klüsener et al., 2002; Allen et al., 1999). Ca^{2+} dependent pathways have been quantified to be responsible for 70% of the ABA response (Siegel et al., 2009). Many independent lines of research have shown activation of stomatal closing mechanisms by increased intracellular $[Ca^{2+}]$ (e.g. Schroeder and Hagiwara, 1989; Grabov and Blatt, 1998; MacRobbie, 2000; Mori et al., 2006; Vahisalu et al., 2008; Siegel et al., 2009). However, the specificity of the signaling components are not well understood. For example, in *Vicia faba* guard cells, there were increases in intracellular $[Ca^{2+}]$ upon addition of ABA (Grabov and Blatt, 1998). However, there were also spontaneous intracellular $[Ca^{2+}]$ transients without exogenous addition of ABA observed in Arabidopsis guard cells (Young et al., 2006, Allen et al., 1999; Klüsener et al., 2002). It has been shown that calcium transients can be further dampened or decreased with either the removal of calcium in the buffer or depolarization

of guard cells (Grabov and Blatt, 1998; Staxen et al., 1999; Klüsener et al., 2002; Young et al., 2006). However, the specificity and plasticity of intracellular $[Ca^{2+}]$ is not known.

There have been a number of theories on the effect of Ca^{2+} on the ABA signaling pathway. Research suggests that stomata can continually show calcium transients in non-stimulated guard cells (Allen et al., 1999; Grabov et al., 1998; Klüsener et al., 2002, Staxen et al., 1999; Yang et al., 2008; Young et al., 2006; Kim et al., 2010), leading to the model that stomatal closure by $[Ca^{2+}]_{cyt}$ requires the simultaneous presence of a stimulus such as ABA or CO_2. This calcium sensitivity priming hypothesis suggests that ABA "primes" the guard cells to detect the (spontaneous) calcium transients, which leads to stomatal closure (Hubbard et al., 2012).

The ABA signaling network in *Arabidopsis thaliana* has both calcium-dependent and -independent pathways. To date, the effect of intracellular $[Ca^{2+}]$ on other components of the ABA signaling pathway is not well understood (Hubbard, 2012). However, understanding the effects of Ca^{2+} on other protein families in the ABA signaling pathway could be important to understanding the role and regulation of Ca^{2+} in stomatal closure and, more specifically, the calcium channel, I_{ca}.

In my thesis, I conducted experiments to test the effect of ABA on PP2C mutants in A. *thaliana* to investigate the core ABA signaling pathway. Next, I tested the effect of Ca^{2+} on the PP2C mutants in A. *thaliana* to elucidate the role of PP2Cs in the calcium dependent ABA pathway. Furthermore, I have tested the effect of Ca^{2+} on PYR/PYL mutants and monitored calcium levels in the presence of ABA in the PYR/PYL mutants using a FRET-based biosensor in A. *thaliana* to understand the role of the START proteins in $[Ca^{2+}]_{cyt}$ regulation.

1.3. Results

1.3.1. Stomatal movement bioassay of abi1-2/abi2-2/pp2ca-1/hab1-1

For figure 1, the "blending" method was used to measure the stomata after exposure to 10 µM ABA. Plants were grown and the abaxial epidermal side of rosettes were incubated in opening buffer (5 mM KCl, 50 µM $CaCl_2$, 10 mM MES, pH 5.6 Tris-base) for 3 hours and then exposed to 10 µM ABA for 1 hour before measurements. These experiments were conducted as double blind for the genotype and treatment used and triplicates were performed on the same day.

According to the results (Figure 1), there was ~40% stomatal closure in Col (wild-type) and ~50% stomatal closure in the *abi1-2/abi2-2/pp2ca-1/hab1-1* mutant. These results are consistent with phosphatase mutant's hypersensitivity to ABA (Kuhn et al., 2006; Rubio et al., 2009). Although there was a high p-value of 0.13, showing no significant difference between wildtype and the *abi1-2/abi2-2/hab1-1/pp2ca-1* mutant, multiple repeats of this experiment showed similar results.

The tracking method was used for the Ca^{2+}-induced time-resolved stomatal tracking bioassay. Experiments were conducted as single blinded with blinded genotype because only one treatment was used (10 mM Ca^{2+}). The rosettes were incubated in opening buffer for 3 hours and 20 stomata were tracked before exposure to 10 mM Ca^{2+} at time points t=0, 10, 30, 60, 120 minutes.

Figure 1: ABA-induced time-resolved stomatal movement bioassay. The abaxial epidermal side of rosette leaves was incubated in opening buffer for 3 hours, and the leaves were incubated in the same opening buffer with 10 μM ABA. **A).** The normalized apertures (normalized to t=0) are graphed. **B).** The actual aperture sizes are graphed. This experiment was repeated three times and the error bars represent ± standard error of three trials. Each trial consisted of 40 stomatal aperture measurements.
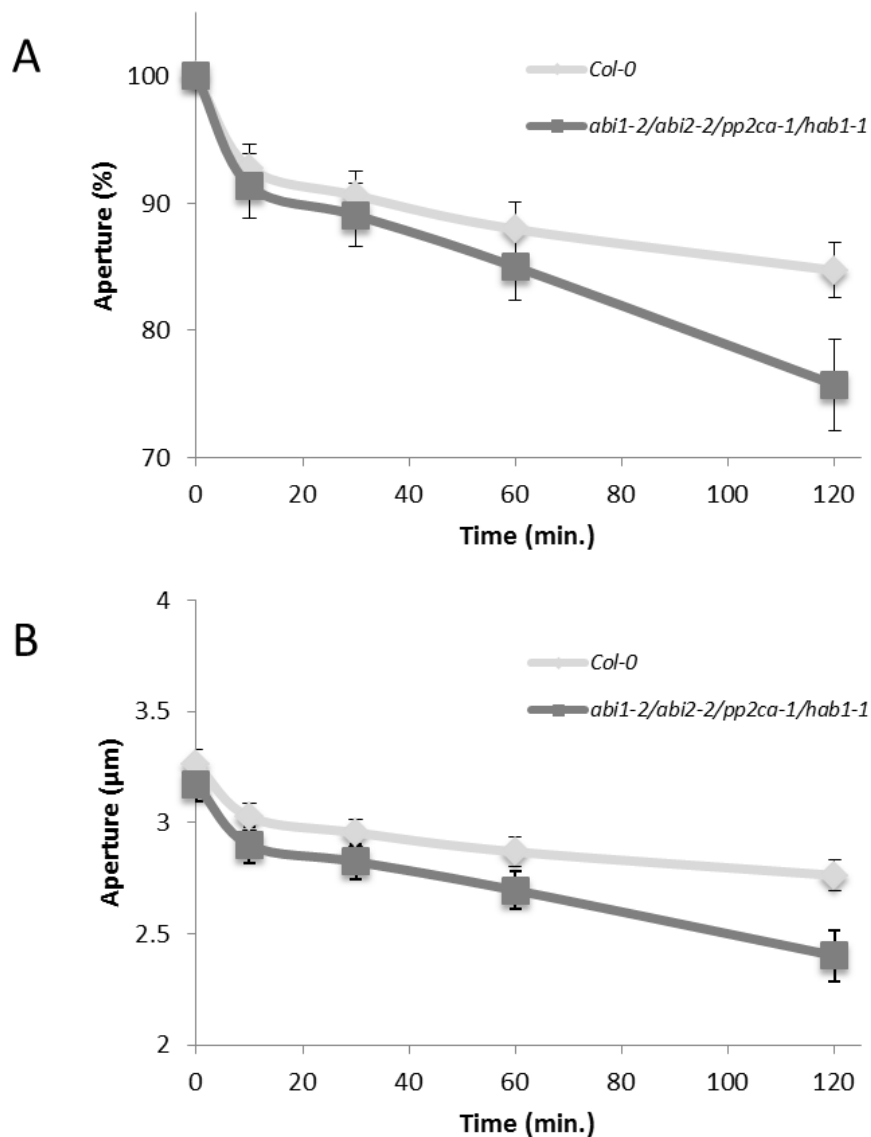
Figure 2: Ca²⁺-induced time-resolved stomatal movement tracking bioassay of *abi1-2/abi2-2/pp2ca-1/hab1-1* mutant. The abaxial epidermal side of rosette leaves was first isolated onto a slide using medical adhesive and a razor blade. The isolated peel was incubated in opening buffer for 3 hours and "tracked" overtime after exposure to 10 mM $CaCl_2$ in opening buffer. Measurements were taken at t=0, 10, 30, 60, 120. **A).** The normalized aperture were graphed depending on the aperture at t=0. **B).** The actual stomatal apertures were graphed. Experiments were single blind experiments and triplicates were performed on the same day. Error bars represent ± standard error of three trials. Each trial consisted of 20 stomata.

1.3.2. Stomatal movement bioassay of pyr1/pyl1/pyl2/pyl4 mutant

The "blending" technique was used to test the effect of 10 mM Ca^{2+} on the *pyr1/pyl1/pyl2/pyl4* quadruple mutant. The same protocol (Materials and Methods) that was used for the PP2C quadruple mutant was used for the PYR/PYL quadruple mutant.

The results showed ~20% closure in WT and ~20% closure in the PYR/PYL quadruple mutant. There was no difference in the normalized or the actual stomatal aperture upon expopsure of ABA. In this set of experiments, further experiments would be needed to substantiate this result.
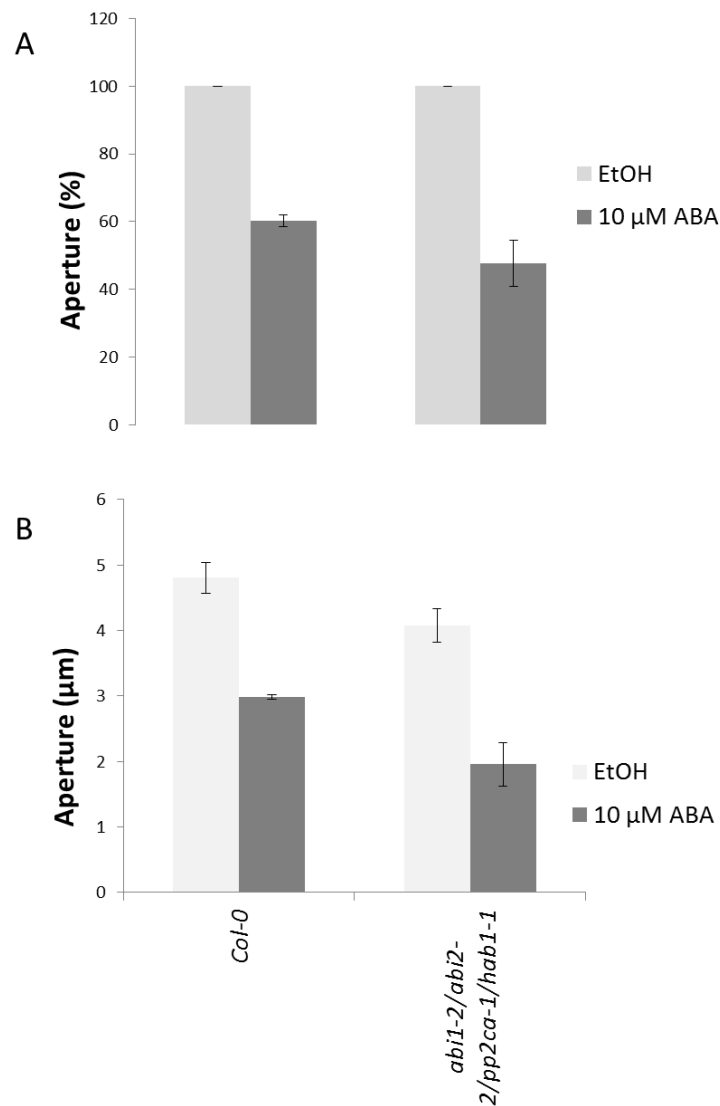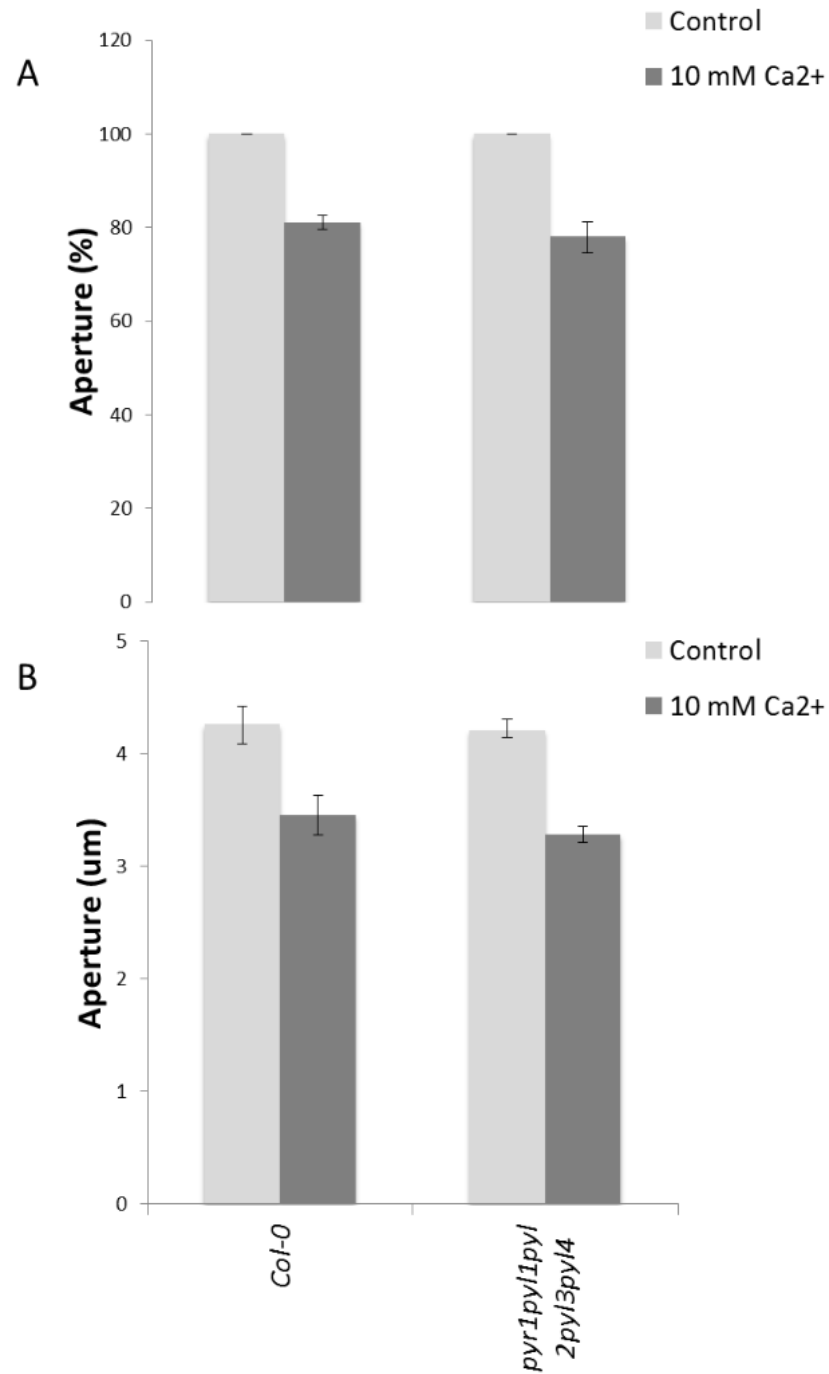
Figure 3: Ca²⁺-induced time-resolved stomatal movement bioassay. The abaxial epidermal side of rosette leaves was incubated in opening buffer for 3 hours, and the leaves was incubated in the same opening buffer with 10 mM $CaCl_2$. **A).** The normalized apertures (normalized to t=0) are graphed **B).** The actual aperture sizes are graphed. This experiment was repeated three times and the error bars represent ± standard error of three trials. Each trial consisted of 40 stomata.

### 1.3.3. ABA-induced Ca^{2+} imaging in guard cells

Yellow cameleon, YC3.6, is a FRET-based sensor that detects changes in Ca^{2+} in real-time (Miyawaki et al., 1997; Miyawaki et al., 1999; Mori et al., 2006). YC3.6 was transformed into *Col* and *pyr1pyl1pyl2pyl4* plants using the pGC1 promoter (Yang et al., 2008). Plants that highly expressed YC3.6 were isolated and grown for Ca^{2+} imaging (Materials and Methods). An excitation filter wheel was set for 440 nm and 475 nm for the CFP and YFP excitation, respectively. The emission filter wheel was set at 480 nm and 535 nm for the CFP and YFP emission, respectively.

The abaxial epidermal tissue of plants were first isolated using medical adhesive and a razor blade. Samples were exposure to opening buffer for 3 hours before the start of experiments. Plants were first equilibrated for 20 minutes using opening buffer before induction of 10 µM ABA in opening buffer. Treatments were changed by removing solution with a kimwipe and adding 200 µl of treament solution using a pipet. Solutions were perfused using the same solution every 20 minutes. Finally, after 40 minutes of ABA induction, 10 mM $CaCl_2$ was added to the in opening buffer to elicit a robust control calcium transient response. Ca^{2+} transient peaks were counted using OriginPro graphing software.
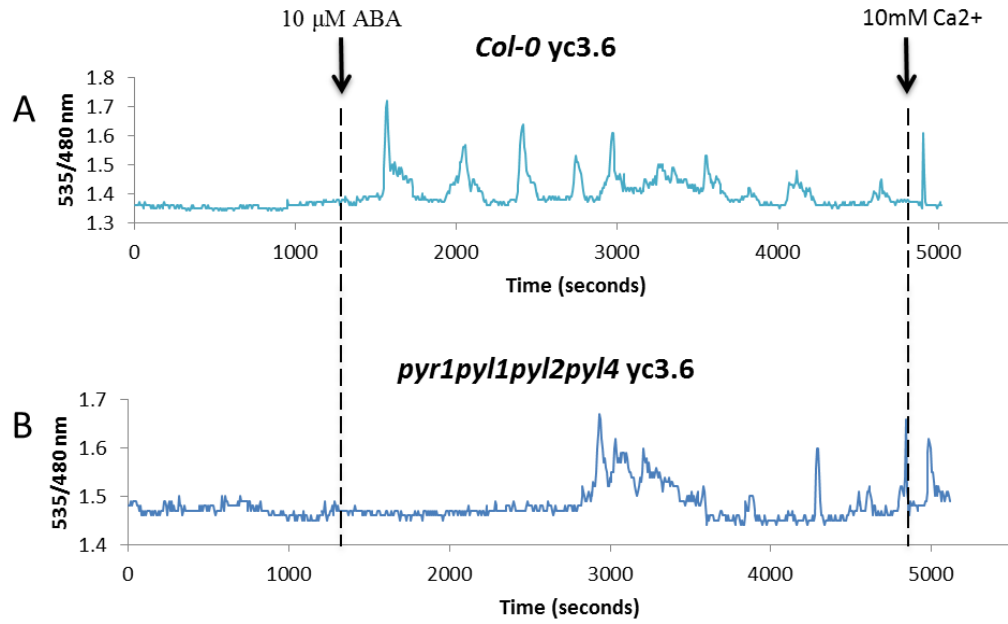
Figure 4: Ratiometric calcium imaging of *pyr1pyl1pyl2pyl4*. The emission at 535 nm and 480 nm were recorded and ratios were taken to measure the $[Ca^{2+}]_{cyt}$ in guard cells. Measurements were taken over a span of 40 minutes and a 10 mM $CaCl_2$ opening buffer was used as a control. (**A**) A single recording for *col* is shown with ABA and Ca^{2+} treatment at specific time points. (**B**) A single recording for *pyr1pyl1pyl2pyl4* is shown.
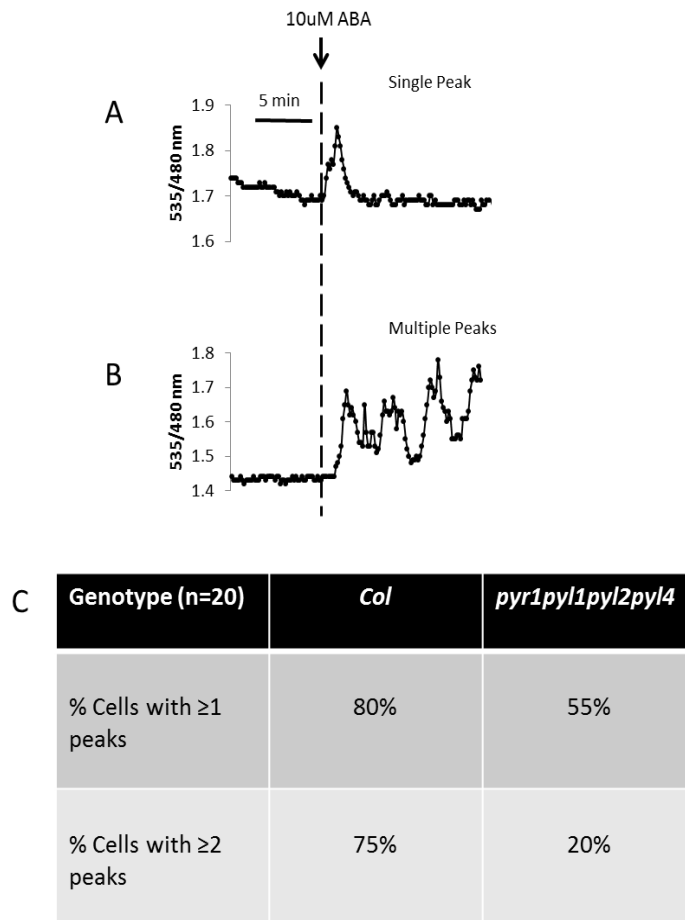
Figure 5: ABA-induced Ca²⁺ transients in guard cells. The occurrence of different Ca^{2+} elevation patterns in guard cells was tabulated for *col* and *pyr1pyl1pyl2pyl4*. The percentage of cells that displayed 1 or more calcium transient peaks were counted and the percentage of cells that displayed 2 or more calcium transient peaks were counted. Both trials used a sample size of n=20. **(A)** Displays an example of an ABA-induced single peak detection in WT. **(B)** An example of multiple peaks upon addition of ABA is shown in WT. **(C)** The result of the % of cells in WT and the mutant are tabulated.

1.4. Discussion

There are many different factors that affect stomatal apertures including: ABA (McAinsh et al., 1990), pathogens (Klüsener et al., 2002), CO_2 (Schwartz, 1985; Yang et al., 2008), ozone (Clayton et al., 1999), reactive oxygen species (ROS) (McAinsh et al., 1996; Pei et al., 2000), external Ca^{2+} (Gilroy et al., 1991; Allen et al., 2001), nitric oxide (Desikan et al., 2002), and other Ca^{2+}-linked stimuli (Leckie et al., 1998; Staxen et al., 1999). Previous data has shown the importance of Ca^{2+} in stomatal closure (Mori et al., 2006; Zhu et al., 2007; Siegel et al., 2009; Hubbard et al., 2012; Kim et al., 2010). All of these stimuli lead to calcium influx and/or organellar Ca^{2+} release in the guard cell. In my thesis work, I have studied the role of PP2Cs and PYR/PYLs in the core ABA signaling pathway and studied their potential relationship to $[Ca^{2+}]_{cyt}$ elevations in signaling.

PP2Cs in the ABA signaling pathway act as negative regulators to inhibit SnRK2 protein kinases. In my thesis, I have shown the effect of ABA (Figure 1) and Ca^{2+} (Figure 2) on the *abi1-2/abi2-2/pp2ca-1/hab1-1* mutant. This specific quadruple pp2c mutant was used because of its large combined role in the ABA signaling pathway. Studies have shown the large role of ABI1 and ABI2 in the ABA pathway (Leung et al., 1994; Leung et al., 1997; Meyer et al., 1994) including: a reduction in ABA-induced calcium elevations (Allen et al., 1999), interaction with PYR/PYL/RCAR families (Nishimura et al., 2010), sensitivity to ABA (Armstrong et al., 1995; Hoth et al., 2002), its role in ROS production (Murata et al., 2001), and, most recently, its direct effect on the SLAC1 channel (Brandt et al., 2012). Additionally, the PP2CA (Kuhn et al., 2006; Yoshida et al., 2006) and HAB1 (Leonhardt et al., 2004; Saez et al., 2004) mutants were used because of their ability to cause a partial ABA response in the absence of ABA in triple mutants,

hab1-1/abi1-2/abi2-2 and *hab1-1/abi1-2/pp2ca-1* (Rubio et al., 2009). Furthermore, pp2ca-1 loss-of-function alleles showed hypersensitivity to ABA (Kuhn et al., 2006; Yoshida et al., 2006), and it has been shown that a hypermorphic mutation in hab1-1 plays a large role in the ABA signaling pathway (Robert et al., 2006). Together, the PP2C quadruple mutant (abi1-2/abi2-2/pp2ca-1/hab1-1) was used to knock out the major functioning phosphatase proteins in the core ABA signaling pathway.

The PP2C quadruple mutant was used to test the effect of ABA and Ca^{2+}. Based on the core ABA signaling model, the PP2Cs function as negative regulators by inhibiting the SnRK2 protein kinases (Umezawa et al. 2009; Vlad et al. 2009) and decreasing SLAC1 anion channel activity. My results show hypersensitivity of the PP2C mutants in the presence of ABA, which supports the model for the ABA signaling pathway. In the absence of the negative regulator, active SnRK2s freely phosphorylate and activate downstream ABA targets such as SLAC1 (Negi et al., 2008; Vahisalu et al., 2008). In my results, there was ~50% closure of the PP2C quadruple mutant and ~40% closure in Col. This difference suggests that ABA functions upstream of the PP2Cs in the ABA signaling pathway as shown in the standing ABA model.

Ca^{2+} has a downstream effect on stomatal aperture in guard cells. It was shown that Ca^{2+} binds with CPKs to regulate downstream events in the ABA pathway (Mori et al., 2006). However, the relationship between Ca^{2+} and PP2Cs is largely unknown. My results showed hypersensitivity of the PP2C quadruple mutant in the presence of Ca^{2+} elevation. After two hours incubation of Ca^{2+}, the PP2C quadruple mutant displayed ~25% closure, while the Col displayed ~15% closure. The larger decrease in aperture from the PP2C quadruple mutant shows that PP2Cs also regulate directly or indirectly to

proteins that are related to calcium-induced activity of proteins. This may be explained by the ability of ABI1 to dephosphorylate and deactivate the SLAC1 channel (Brandt et al., 2012). Furthermore, this could be explained by potential interaction between CPKs and PP2Cs; however, this is still yet to be proven. Overall, PP2Cs may have multiple functions and regulatory mechanisms to closely monitor stomatal aperture by regulating components involved in $[Ca^{2+}]$ regulation.

Next, I studied the effect of Ca^{2+} on the *pyr1/pyl1/pyl2/pyl4* quadruple mutant (Figure 3). PYR1 was used because of its main function as the ABA receptor in the ABA pathway (Nishimura et al., 2009). Using mass spectroscopy, interactors of ABI1 were discovered and a quadruple mutant, py1/pyl1/pyl2/pyl4, was made, which exhibited insensitivity to ABA-induced stomatal closure and ABA-inhibition of stomatal opening (Nishimura et al., 2010). Furthermore, yellow cameleon was transformed into this mutant to monitor calcium elevations in the plant (Miyawaki et al., 1997; Allen et al., 1999) by ratiometric measurements.

Previously, it was shown that the PYR/PYL quadruple mutant showed insensitivity to ABA (Nishimura et al., 2010), so the effect of extracellular Ca^{2+} was tested on the quadruple mutant. Using the downstream effect of extracellular Ca^{2+}, it was shown that WT and the quadruple mutant showed similar stomatal closure, ~20%. Showing that Ca^{2+} acts further downstream of PYR/PYL in the core ABA signaling pathway. The results of the time-resolved stomatal bioassay of the PYR/PYL quadruple mutant did not show any significant results on the mutant's relationship with downstream calcium events; however, these results did not suggest any regulatory mechanisms of Ca^{2+} regulation.

After testing the effect of Ca^{2+} on the PYR/PYL mutants, I tested the effect of ABA on calcium elevations in guard cells using yellow cameleon (Figure 4; Figure 5). The use of YC3.6 allowed $[Ca^{2+}]_{cyt}$ monitoring. The calcium imaging of the PYR/PYL quadruple mutant showed significantly lower calcium transients and lower number of guard cells that responded to ABA, in comparison to WT. The decreased calcium transients in the PYR/PYL quadruple mutant suggests that the ABA receptor proteins may be involved in the regulation of the Ca^{2+} channels. Research has shown that guard cells display spontaneous calcium influxes and ABA-induced calcium elevations (Allen et al., 1999; Schroeder et al., 1987; Klüsener et al., 2002; Yang et al., 2008; Siegel et al., 2009; Schwartz, 1985; McAinsh et al., 1990; Grabov and Blatt, 1998; MacRobbie, 2000). However, there was a significant difference in the number of cells that had spontaneous calcium transients. Moreover, there was a consistent response to extracellular Ca^{2+} *pyr1/pyl1/pyl2/pyl4* quadruple muant, but not ABA, with the exception of background calcium transients.

The study presented in my thesis could be helpful in determining the regulatory mechanisms Ca^{2+} elevations. The absence of PYR1, PYL1, PYL2, and PYL4 displayed a significantly lower number of calcium transients and ABA-induced calcium elevations. This may suggest that the ABA receptor protein may be crucial for activating and/or regulating the Ca^{2+} elevations

In my thesis, I have tested the effects of ABA and Ca^{2+} on the PP2C quadruple mutant, abi1-2/abi2-2/pp2ca-1/hab1-1. I have found that the quadruple mutant was both hypersensitive to ABA and Ca^{2+}, showing that the PP2Cs could be involved in both upstream interaction with ABA/ABA receptor complexes and downstream Ca^{2+}

regulation by interacting with proteins such as CPKs. I have also tested the effects of ABA and Ca^{2+} on the PYR/PYL quadruple mutant, *pyr1/pyl1/pyl2/pyl4*. My results show that the PYR/PYL quadruple mutant has no effect on downstream effects such as Ca^{2+}; however, they may play a pivotal role in regulating the I_{ca}, which was shown by the calcium imaging data.

1.5. Methods and Materials

1.5.1. Seed sterilization and germination

Seeds were sterilized with 75% ethanol and with a bleach solution (50% bleach, 0.05% Tween-20). Then seeds were washed three times with sterilized H_2O. Sterilized seeds were plated onto ½ MS plates (½ strength Murashige and Skoog basal medium Sigma-Aldrich, M0404, 1% Sucrose, 0.8% phytoagar) and vernalized in dark and 4 °C for 96 hours. Plates were then placed in a growth chamber with 16-hr light/8-hr dark in $70\mu E/m^2$ at 20 °C for 7 days.

1.5.2. Seedling transplantation and growth maintenance

1-week old seedlings were transplanted onto sterile soil (Sungro special Blend Professional Growing Mix, Seba Beach, Alberta, Canada) with ~0.2 mL/g of 0.05% Technigro fertilizer in deionized water. Plants were covered for four days after transplantation to maintain humidity and grown in 16-hr light/8-hr dark in 70 $\mu E/m^2$ for three weeks. Plants were watered once a week and misted twice a day with deionized water.

1.5.3. Stomatal movement blending bioassay

The plants were grown as described above. 4-5 week old plants were tented with Saran wrap 16 hours before the experiment. Whole intact rosette leaves were cut and incubated in opening buffer (5 mM KCl, 50 μM $CaCl_2$, 10 mM MES, pH 5.6 Tris-base) for 3 hours in 21°C under a light source at 100 $\mu E/m^2$. Then rosette leaves were incubated in treatment for 1 hour before measurement in 21°C under a light source at 100 $\mu E/m^2$. Treatment for +/- ABA was dissolved in ethanol and a solvent control was used. For preparation of measurement samples, epidermal cells were isolated by blending leaves in

commercial blender (Waring - Torrington, Conneticut) and filtering through a 100 μm

nylon mesh (EMD Millipore). The residue from the mesh was then dabbed on a

microscope slide with 200 μL of the treatment solution and a microscope slide was

placed over the sample for measurement. Pictures of stomata were taken at 40x

magnification and measured using ImageJ (http://rsb.info.nih.gov/ij/). Each treatment and

genotype was blinded and triplicates were performed on the same day.

1.5.4. Time-resolved stomatal movement tracking bioassay

First the abaxial side of rosette leaves was isolated onto a color-coded slide cover

using glue(Hollister Medical Adhesive #7730) and a razor blade (PAL Quality Industrial

Blades #62-0163) (Mori et al., 2006). Color-coded slide cover was made by marking

three distinct colored lines alternating in color, vertically and horizontally, for tracking

stomata. After isolation of the epidermal tissue, cover slides were attached to an open

hole microscope slide with vacuum grease (Dow Corning: high vacuum grease

#2021846-0807) and incubated in opening buffer for 3 hours before addition of

treatment. Measurements were taken at appropriate time points and at 40x magnification.

Images of stomata were analyzed using ImageJ (http://rsb.info.nih.gov/ij/). Triplicates of

the experiment were performed and the experiment was run with blinded genotypes.

1.5.5. ABA-induced [Ca^{2+}] oscillations

Epidermal peels of *Arabidopsis thaliana* were isolated from 4 to 5 week-old

plants. Leaves were prepared by isolating the abaxial side of rosette leaves by gluing onto

a cover slide (as described in time-resolved stomatal movement tracking bioassay). All

the samples were incubated in a large tissue culture dish for 3-4 hours in 21°C under a

light source at 100 μE/m^2. After three hours, slides were prepared on an open-holed

microscope slide with opening buffer using vacuum grease (Corning) and ratiometric measurements were taken at 60x magnification using a Nikon fluorescent microscope with a Xenon lamp. The measurements were recorded using Metafluor imaging proram. The excitation filter wheel was set at 440 nm and 470 nm for CFP and YFP fluorophores, respectively. The emission filter wheel was set at 480 nm and 545 nm for CFP and YFP fluorophores, respectively. Each sample was recorded every 5 seconds for high resolution calcium imaging. The sample was first equilibrated in opening buffer for 20 minutes and inducted with ABA for 40 minutes, only cells that were stable for the first 20 minutes were used for analysis. After induction of ABA, 10 mM $CaCl_2$ in opening buffer was used as a control to test the viability of the cells.

1.6. References

Allen, G. J., Chu, S. P., Harrington, C. L., Schumacher, K., Hoffmann, T., Tang, Y. Y., Grill, E., & Schroeder, J. I. (2001). A defined range of guard cell calcium oscillation parameters encodes stomatal movements. *Nature, 411*(6841), 1053-1057.

Allen, G. J., Kwak, J. M., Chu, S. P., Llopis, J., Tsien, R. Y., Harper, J. F., & Schroeder, J. I. (1999). Cameleon calcium indicator reports cytoplasmic calcium dynamics in Arabidopsis guard cells. *Plant J, 19*(6), 735-747.

Allen, G. J., Murata, Y., Chu, S. P., Nafisi, M., & Schroeder, J. I. (2002). Hypersensitivity of abscisic acid-induced cytosolic calcium increases in the Arabidopsis farnesyltransferase mutant era1-2. *Plant Cell, 14*(7), 1649-1662.

Armstrong, F., Leung, J., Grabov, A., Brearley, J., Giraudat, J., & Blatt, M. R. (1995). Sensitivity to abscisic acid of guard-cell K+ channels is suppressed by abi1-1, a mutant Arabidopsis gene encoding a putative protein phosphatase. *Proc Natl Acad Sci U S A, 92*(21), 9520-9524.

Brandt, B., Brodsky, D. E., Xue, S., Negi, J., Iba, K., Kangasjarvi, J., Ghassemian, M., Stephan, A. B., Hu, H., & Schroeder, J. I. (2012). Reconstitution of abscisic acid activation of SLAC1 anion channel by CPK6 and OST1 kinases and branched ABI1 PP2C phosphatase action. *Proc Natl Acad Sci U S A, 109*(26), 10593-10598.

Buckler, E. S., Holland, J. B., Bradbury, P. J., Acharya, C. B., Brown, P. J., Browne, C., Ersoz, E., Flint-Garcia, S., Garcia, A., Glaubitz, J. C., Goodman, M. M., Harjes, C., Guill, K., Kroon, D. E., Larsson, S., Lepak, N. K., Li, H., Mitchell, S. E., Pressoir, G., Peiffer, J. A., Rosas, M. O., Rocheford, T. R., Romay, M. C., Romero, S., Salvo, S., Sanchez Villeda, H., da Silva, H. S., Sun, Q., Tian, F., Upadyayula, N., Ware, D., Yates, H., Yu, J., Zhang, Z., Kresovich, S., & McMullen, M. D. (2009). The genetic architecture of maize flowering time. *Science, 325*(5941), 714-718.

Clayton, H., Knight, M. R., Knight, H., McAinsh, M. R., & Hetherington, A. M. (1999). Dissection of the ozone-induced calcium signature. *Plant Journal, 17*(5), 575-579.

Deak, K. I., & Malamy, J. (2005). Osmotic regulation of root system architecture. *Plant J, 43*(1), 17-28.

Desikan, R., Griffiths, R., Hancock, J., & Neill, S. (2002). A new role for an old enzyme: nitrate reductase-mediated nitric oxide generation is required for abscisic acid-induced stomatal closure in Arabidopsis thaliana. *Proc Natl Acad Sci U S A,*

99(25), 16314-16318.

Epstein, E., Norlyn, J. D., Rush, D. W., Kingsbury, R. W., Kelley, D. B., Cunningham, G. A., & Wrona, A. F. (1980). Saline culture of crops: a genetic approach. *Science, 210*(4468), 399-404.

Geiger, D., Scherzer, S., Mumm, P., Marten, I., Ache, P., Matschi, S., Liese, A., Wellmann, C., Al-Rasheid, K. A., Grill, E., Romeis, T., & Hedrich, R. (2010). Guard cell anion channel SLAC1 is regulated by CDPK protein kinases with distinct Ca2+ affinities. *Proc Natl Acad Sci U S A, 107*(17), 8023-8028.

Geiger, D., Scherzer, S., Mumm, P., Stange, A., Marten, I., Bauer, H., Ache, P., Matschi, S., Liese, A., Al-Rasheid, K. A., Romeis, T., & Hedrich, R. (2009). Activity of guard cell anion channel SLAC1 is controlled by drought-stress signaling kinase-phosphatase pair. *Proc Natl Acad Sci U S A, 106*(50), 21425-21430.

Gilroy, S., Fricker, M. D., Read, N. D., & Trewavas, A. J. (1991). Role of Calcium in Signal Transduction of Commelina Guard Cells. *Plant Cell, 3*(4), 333-344.

Grabov, A., & Blatt, M. R. (1998). Membrane voltage initiates Ca2+ waves and potentiates Ca2+ increases with abscisic acid in stomatal guard cells. *Proc Natl Acad Sci U S A, 95*(8), 4778-4783.

Himmelbach, A., Iten, M., & Grill, E. (1998). Signalling of abscisic acid to regulate plant growth. *Philos Trans R Soc Lond B Biol Sci, 353*(1374), 1439-1444.

Hoth, S., Morgante, M., Sanchez, J. P., Hanafey, M. K., Tingey, S. V., & Chua, N. H. (2002). Genome-wide gene expression profiling in Arabidopsis thaliana reveals new targets of abscisic acid and largely impaired gene regulation in the abi1-1 mutant. *J Cell Sci, 115*(Pt 24), 4891-4900.

Hubbard, K. E., Siegel, R. S., Valerio, G., Brandt, B., & Schroeder, J. I. (2012). Abscisic acid and CO2 signalling via calcium sensitivity priming in guard cells, new CDPK mutant phenotypes and a method for improved resolution of stomatal stimulus-response analyses. *Ann Bot, 109*(1), 5-17.

Ingram, J., & Bartels, D. (1996). The Molecular Basis of Dehydration Tolerance in Plants. *Annu Rev Plant Physiol Plant Mol Biol, 47*, 377-403.

Kim, T. H., Bohmer, M., Hu, H., Nishimura, N., & Schroeder, J. I. (2010). Guard cell signal transduction network: advances in understanding abscisic acid, CO2, and Ca2+ signaling. *Annu Rev Plant Biol, 61*, 561-591.

Klusener, B., Young, J. J., Murata, Y., Allen, G. J., Mori, I. C., Hugouvieux, V., &

Schroeder, J. I. (2002). Convergence of calcium signaling pathways of pathogenic elicitors and abscisic acid in Arabidopsis guard cells. *Plant Physiol, 130*(4), 2152-2163.

Kuhn, J. M., Boisson-Dernier, A., Dizon, M. B., Maktabi, M. H., & Schroeder, J. I. (2006). The protein phosphatase AtPP2CA negatively regulates abscisic acid signal transduction in Arabidopsis, and effects of abh1 on AtPP2CA mRNA. *Plant Physiol, 140*(1), 127-139.

Laanemets, K., Brandt, B., Li, J., Merilo, E., Wang, Y. F., Keshwani, M. M., Taylor, S. S., Kollist, H., & Schroeder, J. I. (2013). Calcium-Dependent and -Independent Stomatal Signaling Network and Compensatory Feedback Control of Stomatal Opening via Ca2+ Sensitivity Priming. *Plant Physiol*.

Leckie, C. P., McAinsh, M. R., Allen, G. J., Sanders, D., & Hetherington, A. M. (1998). Abscisic acid-induced stomatal closure mediated by cyclic ADP-ribose. *Proc Natl Acad Sci U S A, 95*(26), 15837-15842.

Leonhardt, N., Kwak, J. M., Robert, N., Waner, D., Leonhardt, G., & Schroeder, J. I. (2004). Microarray expression analyses of Arabidopsis guard cells and isolation of a recessive abscisic acid hypersensitive protein phosphatase 2C mutant. *Plant Cell, 16*(3), 596-615.

Leung, J., Bouvier-Durand, M., Morris, P. C., Guerrier, D., Chefdor, F., & Giraudat, J. (1994). Arabidopsis ABA response gene ABI1: features of a calcium-modulated protein phosphatase. *Science, 264*(5164), 1448-1452.

Leung, J., Merlot, S., & Giraudat, J. (1997). The Arabidopsis ABSCISIC ACID-INSENSITIVE2 (ABI2) and ABI1 genes encode homologous protein phosphatases 2C involved in abscisic acid signal transduction. *Plant Cell, 9*(5), 759-771.

MacRobbie, E. A. (1998). Signal transduction and ion channels in guard cells. *Philos Trans R Soc Lond B Biol Sci, 353*(1374), 1475-1488.

MacRobbie, E. A. (2000). ABA activates multiple Ca(2+) fluxes in stomatal guard cells, triggering vacuolar K(+)(Rb(+)) release. *Proc Natl Acad Sci U S A, 97*(22), 12361-12368.

Mcainsh, M. R., Brownlee, C., & Hetherington, A. M. (1990). Abscisic Acid-Induced Elevation of Guard-Cell Cytosolic Ca-2+ Precedes Stomatal Closure. *Nature, 343*(6254), 186-188.

McAinsh, M. R., Clayton, H., Mansfield, T. A., & Hetherington, A. M. (1996). Changes in Stomatal Behavior and Guard Cell Cytosolic Free Calcium in

Response to Oxidative Stress. *Plant Physiol, 111*(4), 1031-1042.

Melcher, K., Ng, L. M., Zhou, X. E., Soon, F. F., Xu, Y., Suino-Powell, K. M., Park, S. Y., Weiner, J. J., Fujii, H., Chinnusamy, V., Kovach, A., Li, J., Wang, Y., Peterson, F. C., Jensen, D. R., Yong, E. L., Volkman, B. F., Cutler, S. R., Zhu, J. K., & Xu, H. E. (2009). A gate-latch-lock mechanism for hormone signalling by abscisic acid receptors. *Nature, 462*(7273), 602-608.

Meyer, K., Leube, M. P., & Grill, E. (1994). A protein phosphatase 2C involved in ABA signal transduction in Arabidopsis thaliana. *Science, 264*(5164), 1452-1455.

Miyawaki, A., Griesbeck, O., Heim, R., & Tsien, R. Y. (1999). Dynamic and quantitative Ca2+ measurements using improved cameleons. *Proc Natl Acad Sci U S A, 96*(5), 2135-2140.

Miyawaki, A., Llopis, J., Heim, R., McCaffery, J. M., Adams, J. A., Ikura, M., & Tsien, R. Y. (1997). Fluorescent indicators for Ca2+ based on green fluorescent proteins and calmodulin. *Nature, 388*(6645), 882-887.

Miyazono, K., Miyakawa, T., Sawano, Y., Kubota, K., Kang, H. J., Asano, A., Miyauchi, Y., Takahashi, M., Zhi, Y., Fujita, Y., Yoshida, T., Kodaira, K. S., Yamaguchi-Shinozaki, K., & Tanokura, M. (2009). Structural basis of abscisic acid signalling. *Nature, 462*(7273), 609-614.

Morgan, J. A. (1984). Interaction of water supply and N in wheat. *Plant Physiol, 76*(1), 112-117.

Mori, I. C., Murata, Y., Yang, Y., Munemasa, S., Wang, Y. F., Andreoli, S., Tiriac, H., Alonso, J. M., Harper, J. F., Ecker, J. R., Kwak, J. M., & Schroeder, J. I. (2006). CDPKs CPK6 and CPK3 function in ABA regulation of guard cell S-type anion- and Ca(2+)-permeable channels and stomatal closure. *PLoS Biol, 4*(10), e327.

Murata, Y., Pei, Z. M., Mori, I. C., & Schroeder, J. (2001). Abscisic acid activation of plasma membrane Ca(2+) channels in guard cells requires cytosolic NAD(P)H and is differentially disrupted upstream and downstream of reactive oxygen species production in abi1-1 and abi2-1 protein phosphatase 2C mutants. *Plant Cell, 13*(11), 2513-2523.

Negi, J., Matsuda, O., Nagasawa, T., Oba, Y., Takahashi, H., Kawai-Yamada, M., Uchimiya, H., Hashimoto, M., & Iba, K. (2008). CO2 regulator SLAC1 and its homologues are essential for anion homeostasis in plant cells. *Nature, 452*(7186), 483-486.

Nishimura, N., Hitomi, K., Arvai, A. S., Rambo, R. P., Hitomi, C., Cutler, S. R.,

Schroeder, J. I., & Getzoff, E. D. (2009). Structural mechanism of abscisic acid binding and signaling by dimeric PYR1. *Science, 326*(5958), 1373-1379.

Nishimura, N., Sarkeshik, A., Nito, K., Park, S. Y., Wang, A., Carvalho, P. C., Lee, S., Caddell, D. F., Cutler, S. R., Chory, J., Yates, J. R., & Schroeder, J. I. (2010). PYR/PYL/RCAR family members are major in-vivo ABI1 protein phosphatase 2C-interacting proteins in Arabidopsis. *Plant J, 61*(2), 290-299.

Park, S. Y., Fung, P., Nishimura, N., Jensen, D. R., Fujii, H., Zhao, Y., Lumba, S., Santiago, J., Rodrigues, A., Chow, T. F., Alfred, S. E., Bonetta, D., Finkelstein, R., Provart, N. J., Desveaux, D., Rodriguez, P. L., McCourt, P., Zhu, J. K., Schroeder, J. I., Volkman, B. F., & Cutler, S. R. (2009). Abscisic acid inhibits type 2C protein phosphatases via the PYR/PYL family of START proteins. *Science, 324*(5930), 1068-1071.

Pei, Z. M., Murata, Y., Benning, G., Thomine, S., Klusener, B., Allen, G. J., Grill, E., & Schroeder, J. I. (2000). Calcium channels activated by hydrogen peroxide mediate abscisic acid signalling in guard cells. *Nature, 406*(6797), 731-734.

Raschke, E., Baumann, G., & Schoffl, F. (1988). Nucleotide sequence analysis of soybean small heat shock protein genes belonging to two different multigene families. *J Mol Biol, 199*(4), 549-557.

Rodrigues, A., Santiago, J., Rubio, S., Saez, A., Osmont, K. S., Gadea, J., Hardtke, C. S., & Rodriguez, P. L. (2009). The short-rooted phenotype of the brevis radix mutant partly reflects root abscisic acid hypersensitivity. *Plant Physiol, 149*(4), 1917-1928.

Rubio, S., Rodrigues, A., Saez, A., Dizon, M. B., Galle, A., Kim, T. H., Santiago, J., Flexas, J., Schroeder, J. I., & Rodriguez, P. L. (2009). Triple loss of function of protein phosphatases type 2C leads to partial constitutive response to endogenous abscisic acid. *Plant Physiol, 150*(3), 1345-1355.

Saez, A., Apostolova, N., Gonzalez-Guzman, M., Gonzalez-Garcia, M. P., Nicolas, C., Lorenzo, O., & Rodriguez, P. L. (2004). Gain-of-function and loss-of-function phenotypes of the protein phosphatase 2C HAB1 reveal its role as a negative regulator of abscisic acid signalling. *Plant J, 37*(3), 354-369.

Santiago, J., Dupeux, F., Round, A., Antoni, R., Park, S. Y., Jamin, M., Cutler, S. R., Rodriguez, P. L., & Marquez, J. A. (2009). The abscisic acid receptor PYR1 in complex with abscisic acid. *Nature, 462*(7273), 665-668.

Santner, A., & Estelle, M. (2009). Recent advances and emerging trends in plant hormone signalling. *Nature, 459*(7250), 1071-1078.

Schroeder, J. I. (1989). Quantitative analysis of outward rectifying K+ channel currents in guard cell protoplasts from Vicia faba. *J Membr Biol, 107*(3), 229-235.

Schroeder, J. I., Kwak, J. M., & Allen, G. J. (2001). Guard cell abscisic acid signalling and engineering drought hardiness in plants. *Nature, 410*(6826), 327-330.

Schroeder, J. I., Raschke, K., & Neher, E. (1987). Voltage dependence of K channels in guard-cell protoplasts. *Proc Natl Acad Sci U S A, 84*(12), 4108-4112.

Schwartz, G. J., & Al-Awqati, Q. (1985). Carbon dioxide causes exocytosis of vesicles containing H+ pumps in isolated perfused proximal and collecting tubules. *Journal of Clinical Investigation, 75*(5), 1638-1644.

Siegel, R. S., Xue, S., Murata, Y., Yang, Y., Nishimura, N., Wang, A., & Schroeder, J. I. (2009). Calcium elevation-dependent and attenuated resting calcium-dependent abscisic acid induction of stomatal closure and abscisic acid-induced enhancement of calcium sensitivities of S-type anion and inward-rectifying K channels in Arabidopsis guard cells. *Plant J, 59*(2), 207-220.

Staxen, I., Pical, C., Montgomery, L. T., Gray, J. E., Hetherington, A. M., & McAinsh, M. R. (1999). Abscisic acid induces oscillations in guard-cell cytosolic free calcium that involve phosphoinositide-specific phospholipase C. *Proc Natl Acad Sci U S A, 96*(4), 1779-1784.

Umezawa, T., Sugiyama, N., Mizoguchi, M., Hayashi, S., Myouga, F., Yamaguchi-Shinozaki, K., Ishihama, Y., Hirayama, T., & Shinozaki, K. (2009). Type 2C protein phosphatases directly regulate abscisic acid-activated protein kinases in Arabidopsis. *Proc Natl Acad Sci U S A, 106*(41), 17588-17593.

Vahisalu, T., Kollist, H., Wang, Y. F., Nishimura, N., Chan, W. Y., Valerio, G., Lamminmaki, A., Brosche, M., Moldau, H., Desikan, R., Schroeder, J. I., & Kangasjarvi, J. (2008). SLAC1 is required for plant guard cell S-type anion channel function in stomatal signalling. *Nature, 452*(7186), 487-491.

Vahisalu, T., Puzorjova, I., Brosche, M., Valk, E., Lepiku, M., Moldau, H., Pechter, P., Wang, Y. S., Lindgren, O., Salojarvi, J., Loog, M., Kangasjarvi, J., & Kollist, H. (2010). Ozone-triggered rapid stomatal response involves the production of reactive oxygen species, and is controlled by SLAC1 and OST1. *Plant J, 62*(3), 442-453.

Vlad, F., Rubio, S., Rodrigues, A., Sirichandra, C., Belin, C., Robert, N., Leung, J., Rodriguez, P. L., Lauriere, C., & Merlot, S. (2009). Protein phosphatases 2C regulate the activation of the Snf1-related kinase OST1 by abscisic acid in Arabidopsis. *Plant Cell, 21*(10), 3170-3184.

Yang, Y., Costa, A., Leonhardt, N., Siegel, R. S., & Schroeder, J. I. (2008). Isolation

of a strong Arabidopsis guard cell promoter and its potential as a research tool. *Plant Methods, 4*, 6.

Yin, P., Fan, H., Hao, Q., Yuan, X., Wu, D., Pang, Y., Yan, C., Li, W., Wang, J., & Yan, N. (2009). Structural insights into the mechanism of abscisic acid signaling by PYL proteins. *Nat Struct Mol Biol, 16*(12), 1230-1236.

Yoshida, T., Nishimura, N., Kitahata, N., Kuromori, T., Ito, T., Asami, T., Shinozaki, K., & Hirayama, T. (2006). ABA-hypersensitive germination3 encodes a protein phosphatase 2C (AtPP2CA) that strongly regulates abscisic acid signaling during germination among Arabidopsis protein phosphatase 2Cs. *Plant Physiol, 140*(1), 115-126.

Young, J. J., Mehta, S., Israelsson, M., Godoski, J., Grill, E., & Schroeder, J. I. (2006). CO(2) signaling in guard cells: calcium sensitivity response modulation, a Ca(2+)-independent phase, and CO(2) insensitivity of the gca2 mutant. *Proc Natl Acad Sci U S A, 103*(19), 7506-7511.

Zhu, S. Y., Yu, X. C., Wang, X. J., Zhao, R., Li, Y., Fan, R. C., Shang, Y., Du, S. Y., Wang, X. F., Wu, F. Q., Xu, Y. H., Zhang, X. Y., & Zhang, D. P. (2007). Two calcium-dependent protein kinases, CPK4 and CPK11, regulate abscisic acid signal transduction in Arabidopsis. *Plant Cell, 19*(10), 3019-3036.

II.

The Development and Characterization

of a FRET-based Malate Sensor

2.1. Abstract

Malate is a metabolite in the TCA cycle and plays an important role in regulating turgor pressure in guard cells. To better understand the *in vivo* fluxes of malate in *Arabidopsis thaliana*, a malate sensor based on Förster resonance energy transfer (FRET) would allow real-time monitoring of malate in plants and other organisms. The malate binding PASp domain , from the two-component system YufLM, was cloned from *Bacillus subtillis* and inserted into a FRET cassette, comprising an mTurquoise and a circular permutated (cp)Venus fluorophore. This sensor was characterized by recording emission/excitation spectra and malate titrations. Furthermore, the substrate specificity and binding affinity of the YufL-based malate sensor was tested by titrating related metabolites.

2.2. Introduction

The discovery of fluorescent proteins and their uses in biology has revolutionized research techniques (Tsien, 1998; Zacharias et al., 2000; Zhang et al., 2002; Okumoto et al., 2012). Both clinical and laboratory research have benefitted from the non-invasive application of fluorescent protein; from protein tagging to detection of cancer, the widely flexible use of fluorescent proteins have allowed new advances in research (Soper et al., 2006; Rodriguez-Mozaz et al., 2004). Furthermore, the research of Tsien, Hellinga, Frommer, and Schroeder have utilized the fluorescent proteins to build Förster Resonance Energy Transfer (FRET)-based biosensors that can be used to monitor molecules *in vivo* in real time (De Lorimier et al., 2002; Tsien et al, 2005; Giepmans et al., 2006).

FRET-based biosensors have become a crucial tool for quantitative analysis of ions, signaling molecules, metabolites, and cellular functions (Okumoto et al., 2012). A well-known Ca^{2+} indicator, yellow cameleon, was discovered to function as a noninvasive tool that accurately measured changes in calcium concentration, in real time, based on the M13, calmodulin-like, binding protein (Miyawaki et al., 1997). The FRET sensor was built by fusing two fluorophores to the end of the N- and C- termini of the M13 protein (Miyawaki et al., 1997). Upon binding to calcium, the protein undergoes a conformational change that elicits a change in the FRET, which is measured by the emission of both fluorophores by taking the ratio of the emission maximums of the accepter fluorophore to the donor fluorophore (Miyawaki et al., 1997). This research tool was utilized for measuring fluxes in Ca^{2+} in Arabidopsis (Miyawaki et al., 1999) and, later, in guard cells (Allen et al., 1999).

Malate is a 4-carbon, dicarboxylic acid in the TCA cycle that is important for plant metabolism and homeostasis (Finkemeier and Sweetlove, 2009). The diversity of malate transport proteins in the *Arabidopsis thaliana* have shed light on the important roles of the metabolite (Martinoia and Rentsch, 1994) and real time cell monitoring may prove to be useful for understanding the physiological role of malate in plants.

In guard cells, it was shown that high CO_2 levels lead to increased levels of cytosolic malate (Hedrich et al., 1994). Also, the presence of malate can induce stomatal closure (Lee et al., 2008). Mutation of the slow anion channel, SLAC1, (Negi et al., 2008; Vahisalu et al., 2008) causes malate accumulation in guard cells (Negi et al.,2008. The SLAC1 channel encodes a distant homologue of bacterial dicarboxylate/malate transporters (Negi et al., 2008; Vahisalu et al., 2008). However the guard cell membrane malate transporter, transporter's specificity, and regulatory mechanisms are not understood and SLAC1 appears not to be highly permeable to malate (Laanemets et al., 2013). The synthesis of a malate FRET-based biosensor would help elucidate the role of malate in plants.

The design of a FRET –based biosensor was based on a protein domain that would bind to malate with high specificity and affinity; and upon binding, would undergo a conformational change for FRET to occur (Hellinga and Marvin, 1998). For building the malate sensor, two bacterial substrate binding proteins (De Lorimier et al., 2002) from *Escherichia coli* and *Bacillus subtillis,* were chosen for potential use as biosensors, DcuS (Zientz et al., 1998) and YufL (Tanaka et al., 2003), respectively. These two proteins were chosen as candidates because of their function to regulate organic acid uptake (Zientz et al., 1998; Golby et al., 1999; Tanaka et al., 2003; Doan et al., 2003). YufL

induces expression of MaeN, a Na^+-coupled malate transporter in the presence of malate (Wei et al., 2000). The substrate binding sites of the PASp domains from both proteins were isolated and fused with a mTurquoise fluorophore (Goedhardt et al., 2010) on the N terminus and a cpVenus fluorophore (Griesbeck et al., 2001) on the C terminus.

In this study, I purified and analyzed the two potential biosensors and detected ratio changes for one of the candidates, the YufL-based biosensor, *in vitro*. Next, I determined the malate binding affinity of the sensor and identified other potential metabolites that would bind to the sensor protein. Citrate was found to bind to the sensor to a relatively high degree compared to other metabolites; however, it was shown that the affinity for citrate was 5 times lower than malate proving the specificity and affinity of the sensor protein could be ideal for future use.

2.3. Results

2.3.1. Initial purification and spectra of two sensor candidates

The two candidate sensors were expressed and purified in *E. coli*. Next, the emission spectra of the DcuS-, YufL-based sensors, and empty control were taken. It was shown that the YufL-based sensor in the presence of 9 mM malate showed a shift in the emission peak of both mTurquoise and cpVenus. After analyzing the spectra, the YufL-based sensor (malate sensor) was then further characterized.
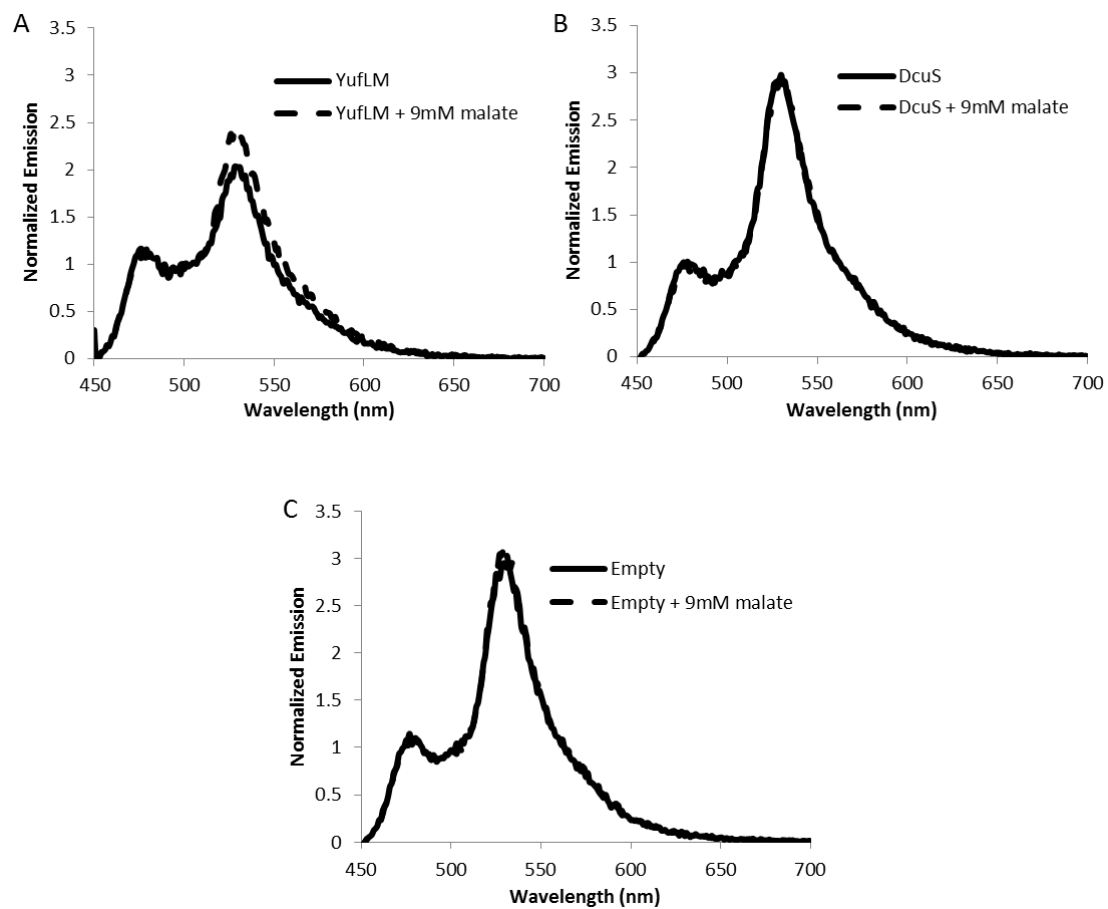
Figure 6: Emission spectra of purified sensor protein from YufL-based sensor, DcuS-based sensor, and an empty sensor control. The sensor protein without malate is shown as a solid line. The dotted line represents the spectra with 9 mM malate.

2.3.2. Expression and purification of malate sensor protein from E. coli

Expression vectors and E. coli strains were cloned and transformed by Hans-Henning Kunz. The malate sensor was built by fusing a mTurquoise fluorophore to the N terminus of the YufL domain and an cpVenus fluorophore bound to the C terminus of the sensor protein. The Strep-tag was placed on the C terminus and used for protein purification (Okumoto et al., 2010). An empty FRET cassette was expressed and purified in parallel and used as a control in all malate sensor assays.

The E. *coli* strain, Rosetta, was used for expression of the sensor protein for purification. Cells were grown until OD_{600} of 0.5 and cells were induced at room temperature for 4 hours using IPTG. The cultures were then lysed and the supernatant was collected for purification using Strep tag. Streptactin Macroprep resin was incubated with the supernatant for 1 hour and loaded onto a Biorad chromatography column for elution.

After the purification of the protein, collected samples were run on an SDS-PAGE gel to determine the quality of the protein purification. As shown in the Figure 2 there was a high level or purity obtained in the elution sample due to the single band present in the brilliant blue stain. This is indicative of a successful purification.
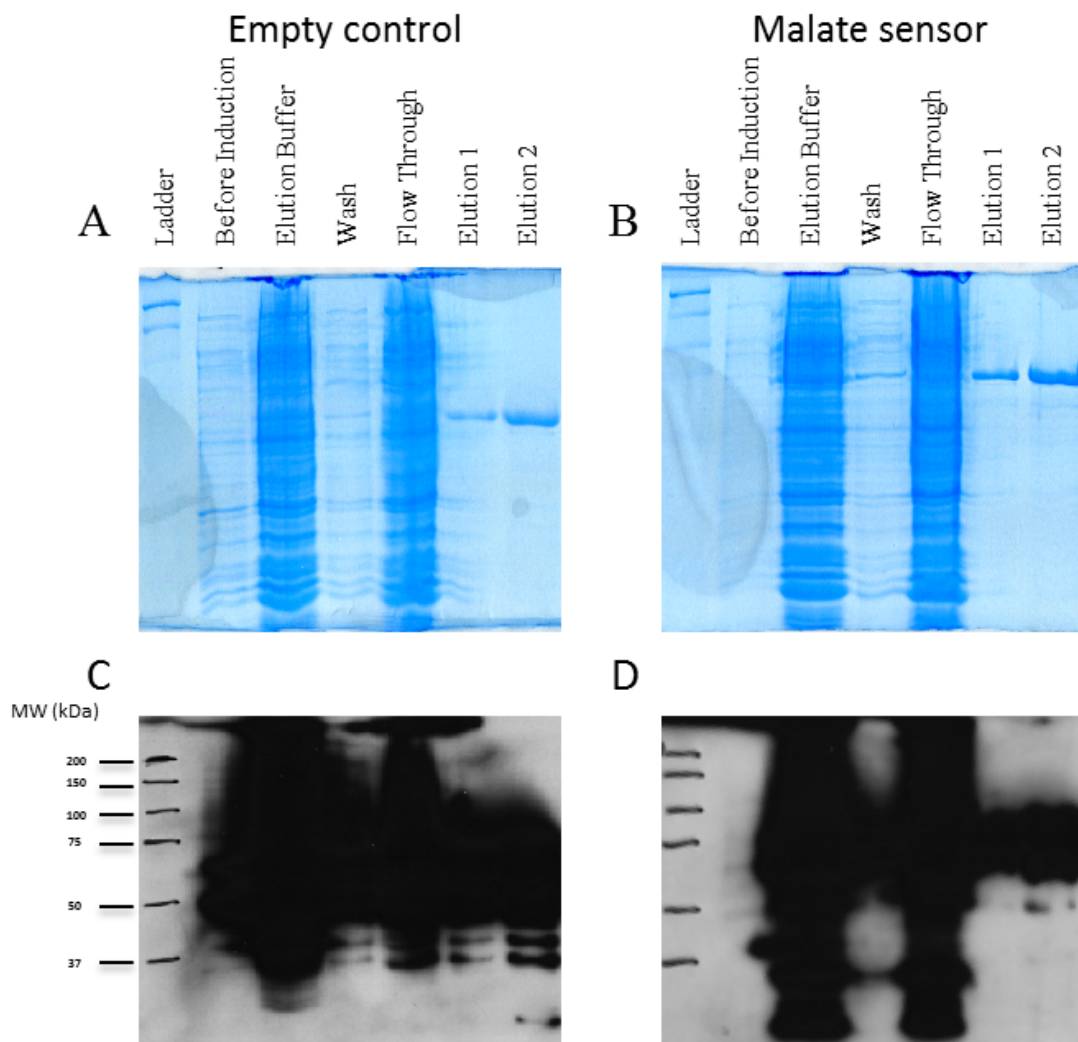
Figure 7: Protein purification from E. *coli* using strep tag. Samples were collected during the protein purification and run on a gel for a brilliant blue protein stain and western blot using a sheep anti rabbit IgG primary antibody for detection of GFP. Samples were loaded on the gel in the same order for all figures. **A and C)** Brilliant blue staining and western blot of empty control, respectively. **B and D)** Brilliant blue staining and western blot of malate sensor, respectively.

.

2.3.3. Excitation and emission spectra of purified sensor

The emission and excitation spectra were recorded for the purified empty control and the malate sensor protein. The overlay of the excitation and emission scan showed that the mTurquoise and ECYP fluorescent proteins were purified. The mTurquoise and cpVenus excitation peaks were 434 and 515 nm and the emission peaks were 480 and 538 nm, respectively (as shown in Figure 3).

The known molar absorptivities of mTurquoise and cpVenus were used to calculate the concentration of the purified protein sample (Table 1) and the ratio of the cpVenus and mTurquoise peak were compared to determine the purity of the sample. A ratio of the two fluorescent protein maxes (cpVenus/mTurquoise) of 2.67 is indicative of equal concentration of both fluorescent proteins, calculated from the molar absorptivity. For the malate sensor purification, a ratio of 3.94 was obtained and the empty control had a ratio of 3.65. The large cpVenus peak might indicate the presence of degraded proteins that were co-purfiied using the strep tag, which was localized on the C terminus next to the cpVenus fluorophore. The higher cpVenus signal can be also explained by the background FRET that occurs without the presence of a substrate.

The emission spectra of the empty control and malate sensor were normalized to 514 nm (the wavelength between the two fluorophore maximas). This allowed comparison of the two peaks of the purified protein (Figure 4). The malate sensor displayed a higher mTurquoise peak and a lower cpVenus peak compared to the empty control. The initial spectra, before addition of any substrate, showed potential for a putative ratio change.
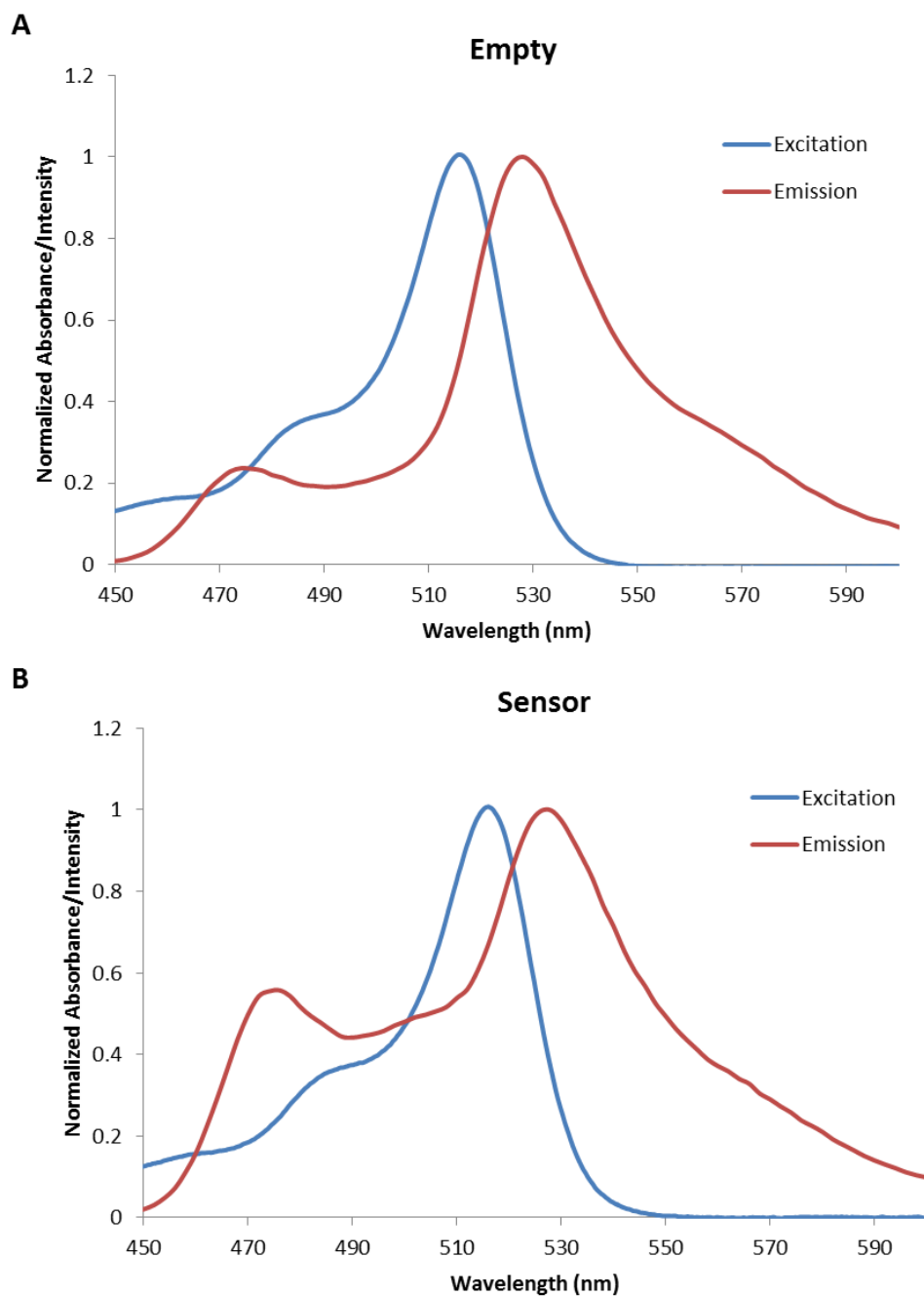
Figure 8: Excitation and emission spectra of purified protein. 100 μL of a 1:100 dilution of purified protein samples were run on a fluorimeter and spectrophotometer to characterize the excitation and emission spectra and to determine the concentration of the protein.

Table 1: Molar absorptivities of purified proteins. The table above lists the molar absorptivities and λ_{max} of mTurquoise (Goedhart et al., 2012) and cpVenus (Nagai et al., 2002).

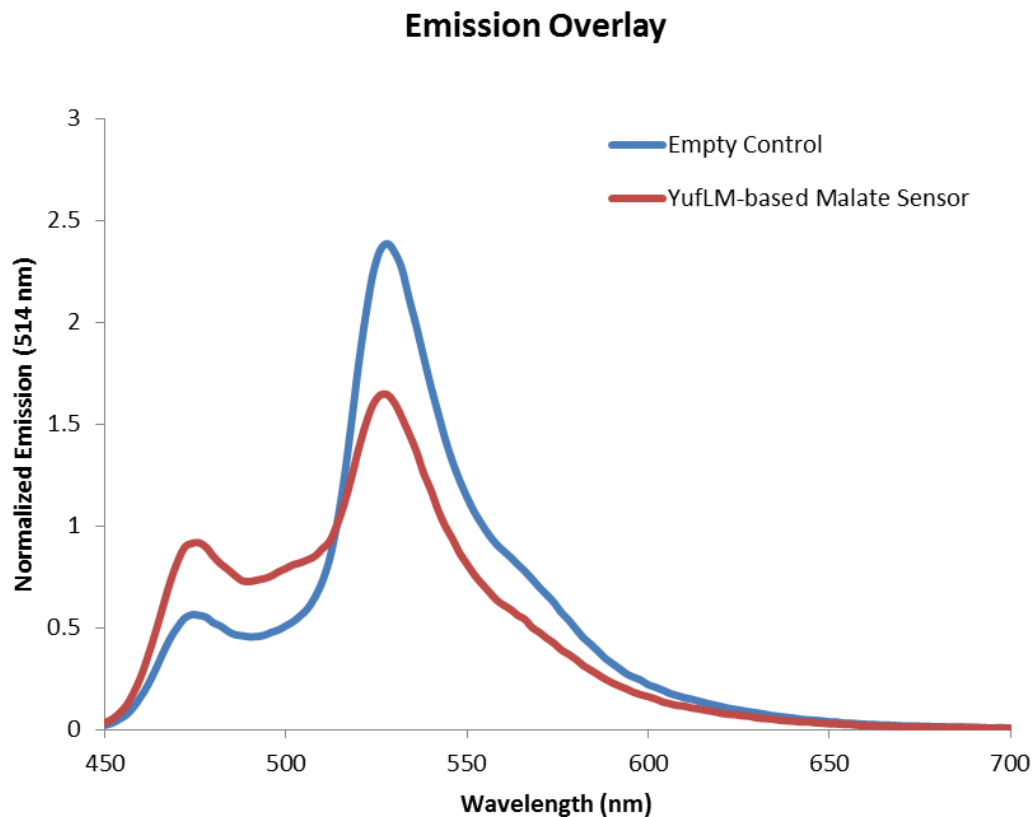| Fluorophore	Molar Absorptivity ($M^{-1}cm^{-1}$)	λ_{nm}
mTurquoise	30,000	434
EYFP	80,000	515

Emission Overlay

Figure 9. Emission spectra of sensors. The emission spectra of the control and malate sensor were graphed together. The graph was normalized to 514 nm, which is the median of the two emission maxes for mTurquoise and cpVenus, 480 nm and 528 nm respectively.

2.3.4. Malate titrations of sensor

In the presence of malate, the empty control did not display any changes in the spectra (Figure 5a). However, the malate sensor showed significant changes in the emission spectra (Figure 5b). From 900 uM to 90 mM, there was a significant change in the mTurquoise peak and the cpVenus peak. As a positive sensor, upon binding of the substrate, the two fluorophores underwent a conformational change that brought the two fluorophores closer together. The cpVenus peak increased, while the mTurquoise peak decreased, which results in a higher degree of FRET upon binding of the malate.

The affinity of the malate sensor to malate was determined by calculating the dissociation constant of the sensor protein. This was obtained by calculating the ratio change at each malate concentration and determining the affinity of the malate to the sensor (Figure 6). The dissociation constant was calculated using Sigmaplot with the equation: $f(x) = minimum + \frac{maximum - minimum}{[1 + \frac{x}{Kd\prime}^{(-Hillslope)}]}$. It was determined that the malate sensor had a K'$_d$ of 1.6 mM^{-1} and a ratio change of 39.4%.
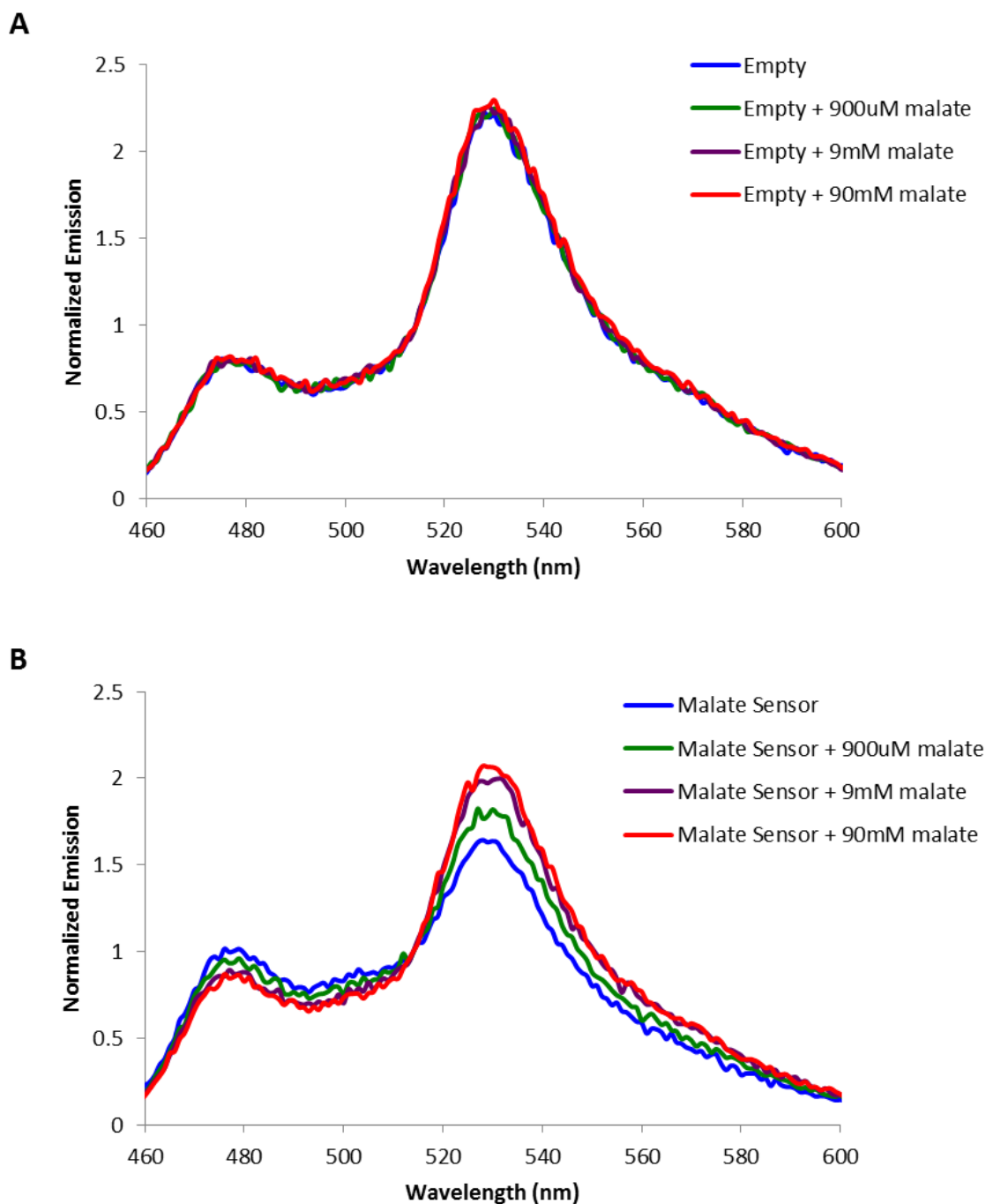
Figure 10. Malate titrations of malate sensor. Purified proteins were diluted to 100 nM and titrated using increasing malate concentrations from 900 μm – 90 mM. All data were recorded in a TECAN Infinite plate reader. Resulting spectra are presented in an overlayto show the change in the mTurquoise and cpVenus emission peaks.
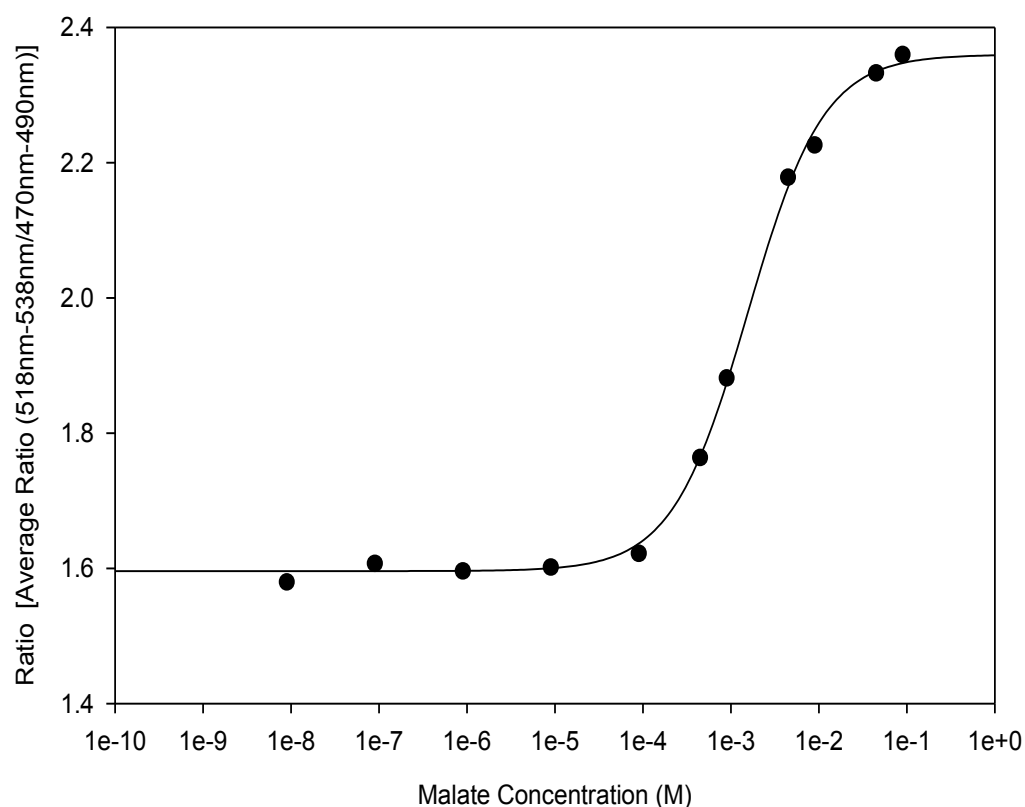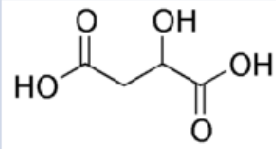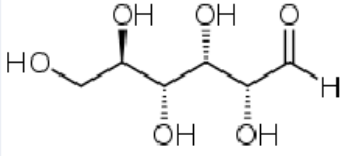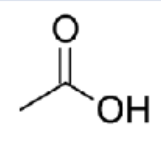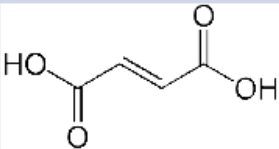
Figure 11: Malate titrations on YufL-based malate sensor protein. The purified protein was diluted into a 100 nM final concentration with increasing malate concentrations in wash buffer II (seen in material and methods). The K'_d was calculated to be 1.6 mM^{-1}. The lowest ratio (528/480nm) was 1.58 and the highest ratio was 2.61, resulting in a 39.4% ratio change after full saturation.

2.3.5. Specificity of malate sensor

The substrate binding specificity of the malate sensor was tested by using structurally similar and related metabolites. The binding affinities of glucose, ac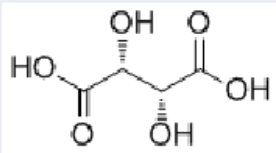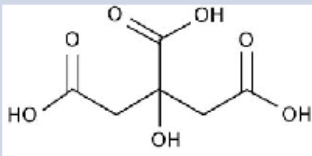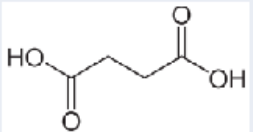etate, tartrate, citrate, fumarate, and succinate were measured by adding 10 mM of each substrate and observing the change in ratio (Figure 7). Structures are given (Table 2). Of all non-malate compunds tested citrate had the highest binding affinity to the sensor protein (Figure 7).

Next, the K'_d of citrate was calculated to be 7.4 mM^{-1} compared to the 1.6 mM^{-1} malate. This shows that the affinity of the malate is approximately 5 fold higher than citrate, which shows that the sensor protein is specific.

Table 2: Molecule structures of compounds tested. Structures of the different metabolites are pictured.

Metabolite	Structure
Malate	
Glucose	
Acetate	
Tartrate	
Citrate	
Succinate	
Fumarate	
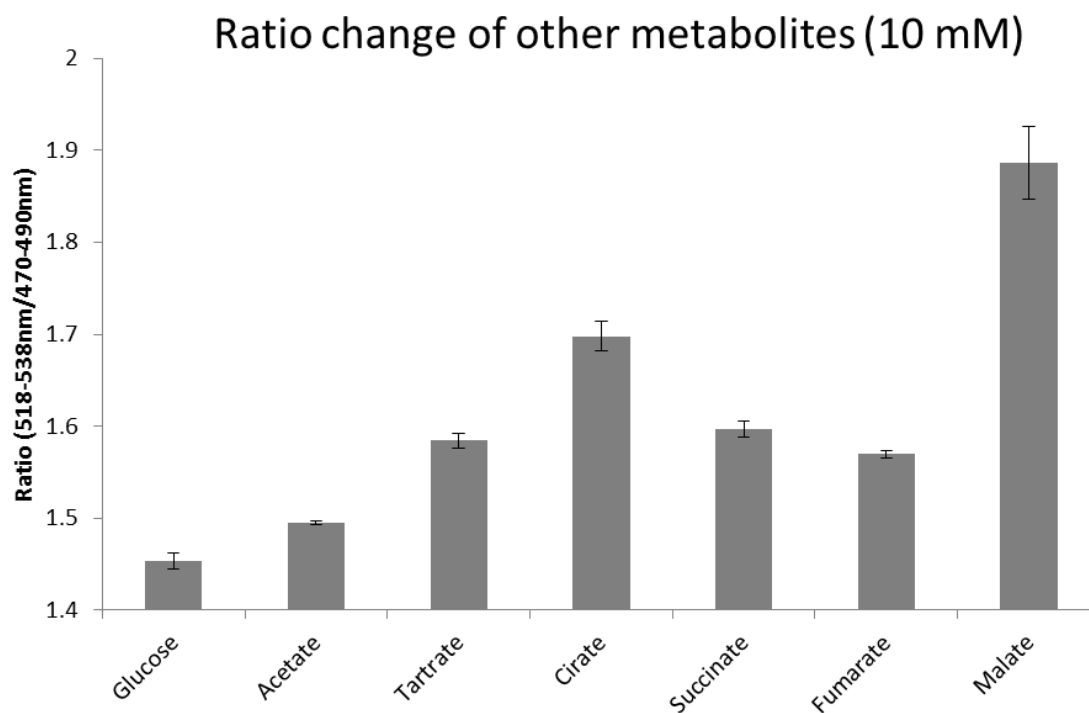
Figure 12: Unspecific binding of YufL-based malate sensor. Indicated metabolites were used to test the unspecific binding of the malate sensor. Ratios were normalized from three replicates of the malate sensor with 0mM malate in wash buffer II. A relatively high affinity to citrate was detected. Error bars represent the standard error calculated from three trials.
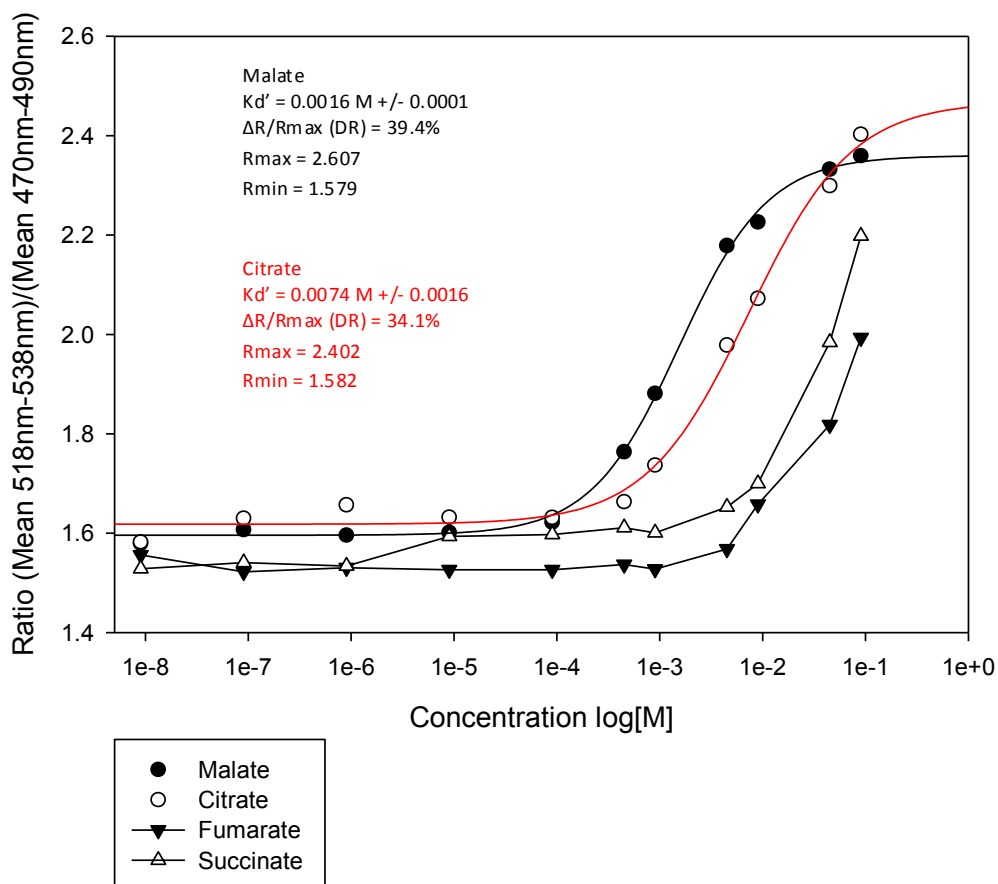
Figure 13: K'_d **of citrate and binding of fumarate and succinate to malate sensor.**
The K'_d of malate and citrate are compared. Fumarate and succinate were used to show
the binding affinities of other TCA metabolites that are structurally-related to malate.
However, only citrate had enough affinity to calculate the K'_d.

2.4. Discussion

FRET-based biosensors allow non-invasive monitoring of metabolites and signal molecules *in vivo*. These biosensors have been successfully used to quantify metabolite fluxes and might be key for future research to discover the roles and fluxes of important molecules (Niittylae et al., 2009, Okumoto et al., 2012). In my thesis, I have worked on characterizing a malate sensor, based on the YufL protein isolated from *B. subtilis*. (Tanaka et al., 2002).

The malate sensor showed a change in emission spectra compared to the DcuS-based sensor and an empty FRET control in the presence of malate. The YufL-based sensor was further characterized because of its ability to undergo a reproducible and robust conformational change that results in a move of the two fluorophores proteins closer together (Figure 1). Both the DcuS-based and empty sensor showed no shift in the presence of malate which rules out the possibility of an unspecific change in ratio by the fluorophores.. After normalizing protein concentrations of the malate sensor and empty protein (Table 1), the emission spectra showed that malate sensor had a higher mTurquoise peak and lower cpVenus peak compared to the empty control indicating the difference in the spatial orientation of the two fluorophores in the absence of malate (Figure 2). The initial shape of the curve showed the potential use of the sensor due to the required fluorescent shift for FRET to occur (De Lorimier et al., 2002; Miyawaki et al., 1997; Ibraheem and Campbell, 2010; Tsien, 1998).

The malate sensor showed robust ratio (528/480nm) changes upon increasing concentration of malate (Figure 5). As the malate concentration increased, the malate sensor underwent conformational change that resembled the spectra of the empty sensor.

This is indicative of a positive sensor because of the decrease in the distance between the two fluorophores upon binding of the ligand and increase in FRET. The type and quality of sensor is determined by the characteristic and size of the linker protein (Hellinga and Richards, 1991; Marvin and Hillinga, 2001). Ideally, showing a large ratio change would allow higher sensitivity for molecule detection. This was shown by other sensors that displayed a large ratio change (Miyawaki et al., 1997; Ewald et al., 2011).

The titration curve and K'_d of the sensor determines the dynamic range at which the sensor could be useful, as well as the affinity between the ligand and protein. In the in vitro experiments, the malate sensor showed a 1 (~39.4%) change in ratio after full saturation of the sensor (Figure 6). The malate sensor showed a dynamic detection range of 100 nM and 100 mM malate. This concentration was based on the affinity of malate towards the native YufL,. One way to change its malate affinity could be achieved by introducing point mutations and modifications into the binding pocket of the YufL protein (Ewald et al., 2011; Miyawaki et al., 1997; Takanaga et al., 2008). Additionally, other metabolites were tested to determine the specificity of the sensor.

The YufL protein was used to build the malate sensor because of its specificity and the structural changes that the protein undergoes upon binding of the ligand (Tanaka et al., 2002). The specificity of a FRET-based sensor is crucial for the integrity of the sensor. So other similar substrates were titrated to show the specificity of the malate sensor (Figure 6). The malate sensor showed very low affinity to many similar metabolites except citrate. The K'_d for citrate was 7.4 mM^{-1} and the 1.6 mM^{-1} for malate showing about a 5-fold increase in the K'_d for citrate. Although citrate had a higher

affinity than other substrates, this sensor still highly favors malate binding because of the high binding affinity of malate (Figure 7; Doan et al., 2003).

Observing ratio changes in the presence of other substrates allowed further characterization of YufL and the specificity of the binding pocket of the YufL protein. By analyzing the structures of the metabolites, the binding pocket of the YufL binding pocket was hypothesized. Malate is a 4 carbon organic acid with a carboxyl group at C1 and C4 position and with a hydroxyl group at the C2 position (Table 2). On the other hand, citrate is a 6 carbon organic acid with a carboxyl group at C1 and C5 position as well as a carboxylmethyl and hydroxyl group at the C3 position (Table 2). These two organic acids show similarities with a carboxyl group adjacent to a hydroxyl group. This shows that the YufL protein specifically binds to the malate organic acid by binding to the C1 and C2 position of malate and the carboxylmethyl functional group of citrate. Moreover, the achiral structure of citrate shows the flexibility of the molecule and possibly explains the stability in the binding pocket of the malate sensor. However, malate most closely resembles tartrate, which only has an additional hydroxyl group at the C3 position. Although tartrate is similar to malate, there is very little binding of tartrate to the sensor. This is most likely due to the steric hindrance that the C3 hydroxyl group causes in the binding pocket of the YufL. This is further supported by citrate's lack of large functional groups adjacent to the hydroxyl group. The YufL specificity is most depended on a carboxyl group with an adjacent hydroxyl group without large molecules on the third carbon position.

In conclusion, this malate FRET biosensor is robust and shows high affinity and specificity for malate as shown by the high ratio change. Future experiments would be to

optimize the sensor to increase the affinity of malate and decrease the affinity of other

substrates such as citrate. Also, it would be important to test other metabolites and basic

molecules, such as glycolic acid, to further test the specificity of the malate sensor.

Finally, an *in vivo* system and assay has to be established for future research and

application of the YufL-based malate sensor.

2.5. Methods and Materials

2.5.1 Expression of Escherichia coli for Purification

E. *coli* expression strain was cloned by Henning Kunz. A 1:100 dilution of selective LB media pre-culture was used to inoculate LB media culture at 37 °C for 2.5-3 hours until OD_{600} of 0.5. Then, the culture was inducted with 0.5mM IPTG. After shaking and incubating at room temperature for 4 hours, the cultures were pelleted and frozen for purification.

2.5.2. Purification of Escherichia coli using strep tag

E. *coli* cells were resuspended in lysis buffer and left on ice for 1 hour. The cells were disrupted by sonication at 20-25% amplitude. The cell lysate was centrifuged and the supernatant was collected and filtered using a 0.45μm syringe. For the purification using the strep tag, the supernatant was incubated with 1:30 dilution of 50% Streptactin$^{©}$ Macroprep and loaded onto the column. The column was washed twice with 10 column volumes of wash buffer I. After the first flow through, the column was washed twice with 10 column volumes of wash buffer I and once with 10 column volumes of wash buffer II. The bound protein was eluted with 3 column volumes of the elution buffer and concentrated to 1 mL using an Amicon Ultra-filter, 30 kDa. Samples were taken for SDS PAGE gel.

2.5.3. Buffers Used for Purification

Lysis buffer: 30 mM Tris/HCl pH 7.4, 250 mM NaCl, 1 mM EDTA, Roche Protease, Inhibitor, 1 mM phenylmethanesulfonylfluoride, 1 mg/mL egg white lysozyme

Wash buffer I: 30 mM Tris/HCl pH 7.4, 250 mM NaCl, 1 mM EDTA

Wash buffer II: 30 mM Tris/HCl pH 7.4**,** 250 mM NaCl

Elution buffer: 30 mM Tris/HCl pH 7.4, 250 mM NaCl, 2.5 mM Desthiobiotin

2.5.4. Brilliant blue strain and western blot of purification

Samples were collected during the purification. Samples were loaded onto a SDS-PAGE gel with SDS-PAGE sample buffer. After transferring the proteins to the PVDF membrane, the SDS-PAGE gel was placed in a brilliant blue staining solution and the membrane was blocked and incubated in a 1:4000 dilution of GFP sheep anti rabbit IgG overnight. Then the membrane was washed and incubated in a secondary antibody for detection using ECL solution and coumaric acid. Pictures of gels were taken using Kodak X-Omat LS film and the SDS-PAGE gel was stored and pictured using cellophane.

2.5.5. Excitation and emission spectra analysis

Emission spectrum for purified proteins was taken using 1:100 dilution of purified protein with a Fluorolog – Jobin Yvon Horiba fluorimeter. Excitation spectrum for purified proteins was taken using 1:100 dilution of purified protein with a UV-2700 UV-VIS Spectrophotometer - Shimadzu. The concentration of protein was measured using the molar absorptivities and excitation maximums of mTurquoise, 30,000 $M^{-1}cm^{-1}$ at 434 nm, and cpVenus, 80,400 $M^{-1}cm^{-1}$ at 528 nm.

2.5.6. Emission spectra for malate titrations

The emission spectra for malate titrations were measured between 450-700 nm using a TECAN Infinite plate reader. Each well contained 100 uL of 100 nM of purified protein in wash buffer II, pH 7.4, with final concentration of substrate. The **K'$_d$** of the substrates were calculated using the equation: $f(x) = minimum + \dfrac{maximum - minimum}{[1 + \frac{x}{Kd\prime}^{(-Hillslope)}]}$ in Sigmaplot.

2.6. References

Allen, G. J., Kwak, J. M., Chu, S. P., Llopis, J., Tsien, R. Y., Harper, J. F., & Schroeder, J. I. (1999). Cameleon calcium indicator reports cytoplasmic calcium dynamics in Arabidopsis guard cells. *Plant J, 19*(6), 735-747.

Davies, S. J., Golby, P., Omrani, D., Broad, S. A., Harrington, V. L., Guest, J. R., Kelly, D. J., & Andrews, S. C. (1999). Inactivation and regulation of the aerobic C-4-dicarboxylate transport (dctA) gene of Escherichia coli. *Journal of Bacteriology, 181*(18), 5624-5635.

De Lorimier, R. M., Smith, J. J., Dwyer, M. A., Looger, L. L., Sali, K. M., Paavola, C. D., Rizk, S. S., Sadigov, S., Conrad, D. W., Loew, L., & Hellinga, H. W. (2002). Construction of a fluorescent biosensor family. *Protein Sci, 11*(11), 2655-2675.

Doan, T., Servant, P., Tojo, S., Yamaguchi, H., Lerondel, G., Yoshida, K., Fujita, Y., & Aymerich, S. (2003). The Bacillus subtilis ywkA gene encodes a malic enzyme and its transcription is activated by the YufL/YufM two-component system in response to malate. *Microbiology-Sgm, 149*, 2331-2343.

Ewald, J. C., Reich, S., Baumann, S., Frommer, W. B., & Zamboni, N. (2011). Engineering genetically encoded nanosensors for real-time in vivo measurements of citrate concentrations. *PLoS One, 6*(12), e28245.

Finkemeier, I., & Sweetlove, L. J. (2009). The role of malate in plant homeostasis. *F1000 Biol Rep, 1*, 47.

Giepmans, B. N., Adams, S. R., Ellisman, M. H., & Tsien, R. Y. (2006). The fluorescent toolbox for assessing protein location and function. *Science, 312*(5771), 217-224.

Goedhart, J., van Weeren, L., Hink, M. A., Vischer, N. O., Jalink, K., & Gadella, T. W., Jr. (2010). Bright cyan fluorescent protein variants identified by fluorescence lifetime screening. *Nat Methods, 7*(2), 137-139.

Goedhart, J., von Stetten, D., Noirclerc-Savoye, M., Lelimousin, M., Joosen, L., Hink, M. A., van Weeren, L., Gadella, T. W., Jr., & Royant, A. (2012). Structure-guided evolution of cyan fluorescent proteins towards a quantum yield of 93%. *Nat Commun, 3*, 751.

Griesbeck, O., Baird, G. S., Campbell, R. E., Zacharias, D. A., & Tsien, R. Y. (2001). Reducing the environmental sensitivity of yellow fluorescent protein. Mechanism and applications. *J Biol Chem, 276*(31), 29188-29194.

Hedrich, R., Marten, I., Lohse, G., Dietrich, P., Winter, H., Lohaus, G., & Heldt, H. W. (1994). Malate-Sensitive Anion Channels Enable Guard-Cells to Sense Changes in the Ambient Co2 Concentration. *Plant Journal, 6*(5), 741-748.

Ibraheem, A., & Campbell, R. E. (2010). Designs and applications of fluorescent protein-based biosensors. *Curr Opin Chem Biol, 14*(1), 30-36.

Laanemets, K., Brandt, B., Li, J., Merilo, E., Wang, Y. F., Keshwani, M. M., Taylor, S. S., Kollist, H., & Schroeder, J. I. (2013). Calcium-Dependent and -Independent Stomatal Signaling Network and Compensatory Feedback Control of Stomatal Opening via Ca2+ Sensitivity Priming. *Plant Physiol*.

Lee, M., Choi, Y., Burla, B., Kim, Y. Y., Jeon, B., Maeshima, M., Yoo, J. Y., Martinoia, E., & Lee, Y. (2008). The ABC transporter AtABCB14 is a malate importer and modulates stomatal response to CO2. *Nat Cell Biol, 10*(10), 1217-1223.

Martinoia, E., & Rentsch, D. (1994). Malate Compartmentation - Responses to a Complex Metabolism. *Annual Review of Plant Physiology and Plant Molecular Biology, 45*, 447-467.

Marvin, J. S., & Hellinga, H. W. (1998). Engineering biosensors by introducing fluorescent allosteric signal transducers: Construction of a novel glucose sensor. *Journal of the American Chemical Society, 120*(1), 7-11.

Miyawaki, A., Griesbeck, O., Heim, R., & Tsien, R. Y. (1999). Dynamic and quantitative Ca2+ measurements using improved cameleons. *Proc Natl Acad Sci U S A, 96*(5), 2135-2140.

Miyawaki, A., Llopis, J., Heim, R., McCaffery, J. M., Adams, J. A., Ikura, M., & Tsien, R. Y. (1997). Fluorescent indicators for Ca2+ based on green fluorescent proteins and calmodulin. *Nature, 388*(6645), 882-887.

Nagai, T., Ibata, K., Park, E. S., Kubota, M., Mikoshiba, K., & Miyawaki, A. (2002). A variant of yellow fluorescent protein with fast and efficient maturation for cell-biological applications. *Nat Biotechnol, 20*(1), 87-90.

Nagai, T., Yamada, S., Tominaga, T., Ichikawa, M., & Miyawaki, A. (2004). Expanded dynamic range of fluorescent indicators for Ca(2+) by circularly permuted yellow fluorescent proteins. *Proc Natl Acad Sci U S A, 101*(29), 10554-10559.

Negi, J., Matsuda, O., Nagasawa, T., Oba, Y., Takahashi, H., Kawai-Yamada, M., Uchimiya, H., Hashimoto, M., & Iba, K. (2008). CO2 regulator SLAC1 and its homologues are essential for anion homeostasis in plant cells. *Nature, 452*(7186),

483-486.

Niittylae, T., Chaudhuri, B., Sauer, U., & Frommer, W. B. (2009). Comparison of quantitative metabolite imaging tools and carbon-13 techniques for fluxomics. *Methods Mol Biol, 553*, 355-372.

Okumoto, S. (2010). Imaging approach for monitoring cellular metabolites and ions using genetically encoded biosensors. *Curr Opin Biotechnol, 21*(1), 45-54.

Okumoto, S., Jones, A., & Frommer, W. B. (2012). Quantitative imaging with fluorescent biosensors. *Annu Rev Plant Biol, 63*, 663-706.

Rodriguez-Mozaz, S., Marco, M. P., Lopez de Alda, M. J., & Barcelo, D. (2004). Biosensors for environmental monitoring of endocrine disruptors: a review article. *Anal Bioanal Chem, 378*(3), 588-598.

Schmidt, C., & Schroeder, J. I. (1994). Anion Selectivity of Slow Anion Channels in the Plasma-Membrane of Guard-Cells - Large Nitrate Permeability. *Plant Physiology, 106*(1), 383-391.

Soper, S. A., Brown, K., Ellington, A., Frazier, B., Garcia-Manero, G., Gau, V., Gutman, S. I., Hayes, D. F., Korte, B., Landers, J. L., Larson, D., Ligler, F., Majumdar, A., Mascini, M., Nolte, D., Rosenzweig, Z., Wang, J., & Wilson, D. (2006). Point-of-care biosensor systems for cancer diagnostics/prognostics. *Biosens Bioelectron, 21*(10), 1932-1942.

Takanaga, H., Chaudhuri, B., & Frommer, W. B. (2008). GLUT1 and GLUT9 as major contributors to glucose influx in HepG2 cells identified by a high sensitivity intramolecular FRET glucose sensor. *Biochim Biophys Acta, 1778*(4), 1091-1099.

Tanaka, K., Kobayashi, K., & Ogasawara, N. (2003). The Bacillus subtilis YufLM two-component system regulates the expression of the malate transporters MaeN (YufR) and YflS, and is essential for utilization of malate in minimal medium. *Microbiology-Sgm, 149*, 2317-2329.

Tsien, R. Y. (1998). The green fluorescent protein. *Annu Rev Biochem, 67*, 509-544.

Tsien, R. Y. (2005). Building and breeding molecules to spy on cells and tumors. *FEBS Lett, 579*(4), 927-932.

Vahisalu, T., Kollist, H., Wang, Y. F., Nishimura, N., Chan, W. Y., Valerio, G., Lamminmaki, A., Brosche, M., Moldau, H., Desikan, R., Schroeder, J. I., & Kangasjarvi, J. (2008). SLAC1 is required for plant guard cell S-type anion channel function in stomatal signalling. *Nature, 452*(7186), 487-491.

Wei, Y., Guffanti, A. A., Ito, M., & Krulwich, T. A. (2000). Bacillus subtilis YqkI is a novel malic/Na(+)-lactate antiporter that enhances growth on malate at low protonmotive force. *Journal of Biological Chemistry, 275*(39), 30287-30292.

Zacharias, D. A., Baird, G. S., & Tsien, R. Y. (2000). Recent advances in technology for measuring and manipulating cell signals. *Curr Opin Neurobiol, 10*(3), 416-421.

Zhang, J., Campbell, R. E., Ting, A. Y., & Tsien, R. Y. (2002). Creating new fluorescent probes for cell biology. *Nat Rev Mol Cell Biol, 3*(12), 906-918.

Zientz, E., Bongaerts, J., & Unden, G. (1998). Fumarate regulation of gene expression in Escherichia coli by the DcuSR (dcuSR genes) two-component regulatory system. *Journal of Bacteriology, 180*(20), 5421-5425.

Appendix

Other ABA-induced time-resolved stomatal bioassays

    a. gles1 mutant shows no phenotype with 10 um ABA

    b. vdac 3-1 showed slight insensitivity to 10 um ABA

    c. vdac 1-2 showed slight insensitivity to 10 um ABA

    d. cipk1/cbl1 in WS ecotype showed no phenotype in the presence of 10 um and 1 um ABA

    e. cipk1/cbl1 in Col ecotype showed no phenotype in the presence of 10 um and 1 um ABA

        i. ost1 in the Ler background shows similar insensitivity to ABA as Col

    f. camta 5-2/6-4 showed similar sensitivity to ABA compared to WT

Other Ca^{2+}-induced time-resolved stomatal bioassays

    a. camta5-2/6-4 showed insensitivities in the presence of Ca^{2+}

        i. camta 5-2 and camta 6-4 did not show synergistic phenotype to the presence of Ca^{2+} compared to single knocks outs.

Other substrate-induced time-resolved stomatal bioassays

    a. almt12-1 and WT seem to respond similarly to 10 uM molic acid

    b. 100 um H2O2 in pp2ca-1 and *pyr1/pyl1/pyl2/pyl4* does not elicit a robust response.